**Title**
HYALURONIC ACID-BASED HYDROGELS AS AN IN VITRO APPROACH TO NEURAL STEM/PROGENITOR CELL DIFFERENTIATION



**Author**
Bierman, Rebecca

**Publication Date**
2018

UNIVERSITY OF CALIFORNIA

Los Angeles

# HYALURONIC ACID-BASED HYDROGELS AS AN *IN VITRO* APPROACH TO NEURAL STEM/PROGENITOR CELL DIFFERENTIATION

A dissertation submitted in partial satisfaction of the

requirements for the degree Master of Science

in Bioengineering

by

Rebecca Dorian Bierman

2018

ABSTRACT OF THE DISSERTATION

# HYALURONIC ACID-BASED HYDROGELS AS AN *IN VITRO* APPROACH TO NEURAL STEM/PROGENITOR CELL DIFFERENTIATION

by

Rebecca Dorian Bierman

Master of Science in Bioengineering

University of California, Los Angeles, 2018

Professor Stephanie Kristin Seidlits, Chair

The central nervous system (CNS) consists of neurons and glia. In the healthy CNS, neurons form connected networks and oligodendrocytes, a type of glial cell, insulate and support the neuronal functions. When a spinal cord injury (SCI) occurs, a second type of glial cell, astrocytes infiltrate the injury site and cause a cascade of changes[1]. As a result, SCI often leads to permanent motor and sensory loss below the injury site[2]. In addition, the individual is faced with a lifetime of medical care ranging from $2.3-4.7 billion[3]. Around 300,000 people are currently living with SCI in the United States, with around 17,7000 new cases per year[3]. This creates a need and opportunity for restorative, rather than assistive, care.

To repair the spinal cord, there are several considerations, including but not limited to, prevention or reversal of the glial scar formation, introduction of exogenous neural cells and stimulation of the repair process of severed axons. To produce lineages of cells that can be used for introduction at the SCI site, it is necessary to culture them first *in vitro.* Neural stem/progenitor cells (NS/PCs) are pluripotent precursor cells that can differentiate into neurons and glia and be cultured outside of the body[4]. Cells have been cultured in 2D environments for over a century[5]; however, technological advances of the late 19$^{th}$ century have provided new techniques to culture cells in a more biomimetic, 3D microenvironment[6,7]. These 3D microenvironments provide a medium to reliably culture cells into desired lineages, such as populations of neurons and oligodendrocytes.

This research focuses on creating hyaluronic acid (HA)-based hydrogels that serve as 3D microenvironments for cultured NS/PCs in which they can proliferate and differentiate. HA is very biocompatible since it is naturally abundant within the human body, including in the spinal cord, as a key component of the extracellular matrix (ECM)[8]. One benefit of HA-based hydrogels is their tunability for different applications[9]. As shown in this research, the chemical and mechanical properties can be manipulated while maintaining the structural integrity of the hydrogel. Specifically, the HA concentration of the hydrogels can be independently assessed to better understand the interactions of HA with the encapsulated cells at different concentrations. NS/PC mechanostranduction of their microenvironment has been shown to produce signaling pathways within the cells with potential consequences on cell survival and growth[10] so, another tunable parameter explored in this research was how NS/PCs respond to the stiffness of the hydrogels. HA has also been shown to reduce glial scar thickness by decreasing the number of astrocytes present after SCI[11]. As indicated, these HA-based hydrogels demonstrate several

advantages as a vehicle for application of differentiated neural cells to the SCI site.

HA provides a hydrated matrix in which cells can migrate, differentiate and communicate with cell membrane receptors on neural cells, such as CD44, RHAMM and ICAM-1 to elicit cascade effects such as morphogenesis, inflammation, wound repair and metastasis[9]. When HA receptors are bound they also cause a relay of biochemical and mechanical information about the microenvironment to effect cascades of intracellular changes[12]. Thus, it is important to understand and dissociate the effects of mechanical (stiffness) and chemical (HA concentration) properties of the hydrogel microenvironment to elucidate the distinct and/or synergistic effects.

The hydrogels produced from this research aimed to test the effects of three different HA concentrations (0.1 wt%, 0.5 wt% and 1 wt%) on the survival, proliferation and differentiation of encapsulated NS/PCs. Another aspect of this project was to test varied mechanical properties of the hydrogels to determine the effect on encapsulated cells. Soft (200 Pascal), medium (400 Pascal) and stiff (800 Pascal) environments were compared, with values closely matched to the elasticity of biological nerve ECM which ranges from 0.5-1 kPa[13]. A 2D control was also compared to the hydrogel conditions to determine relative cell survival, proliferation and differentiation.

Ultimately, this research is useful because it provides the opportunity to understand how the 3D environment alone (relatively no HA), the concentration of HA, and a softer vs. stiffer environment affects NS/PC proliferation and differentiation. The long-term goal of this research is to produce a robust and biocompatible *in vitro* microenvironment that directs differentiation of an enriched population of specific neural cell types, neurons and oligodendrocytes. Future research can then assess the efficacy of injecting the encapsulated neural cells into the SCI site as an approach to therapeutic repair

The thesis of Rebecca Dorian Bierman is approved.

Song Li

Benjamin M Wu

Timothy J Deming

Stephanie Kristin Seidlits, Committee Chair

University of California, Los Angeles

2018

## ACKNOWLEDGEMENTS

Dr. Seidlits for her mentorship and support of this research

Chris Walthers for lessons in cell culture, immunostaining, and hydrogel fabrication

Jesse Liang for his tireless help and answers to all my questions

Weikun Xiao for lessons in how to cryosection hydrogels and run qPCR

Alireza Sohrabi for lessons in rheology and confocal microscopy


## DEDICATION

This thesis is dedicated to my mother, Sylvia. I am deeply grateful for her support of me doing what I love in life.

TABLE OF CONTENTS

# CHAPTER 1: NEURAL STEM/PROGENITOR CELLS

## 1.1 Central Nervous System

Barring sponges and Trichoplax, every multicellular organism relies on neurons to create the electrical activity required to survive[14]. From sensing the environment to complex decision making the nervous system executes the code for survival. The wiring of the human nervous system is comprised of neurons, varying morphology cells that intake chemicals and transduce the energy into electrical conduction. The conduit that surrounds and insulates neurons is a type of glial cell called an oligodendrocyte (Figure 1). A second type of glial cell, astrocytes, support neurons and regulate their extracellular environment by controlling ionic and chemical concentrations[15]. Together these neuronal cell types comprise the human nervous system, and are supplied with nutrients from the bloodstream.

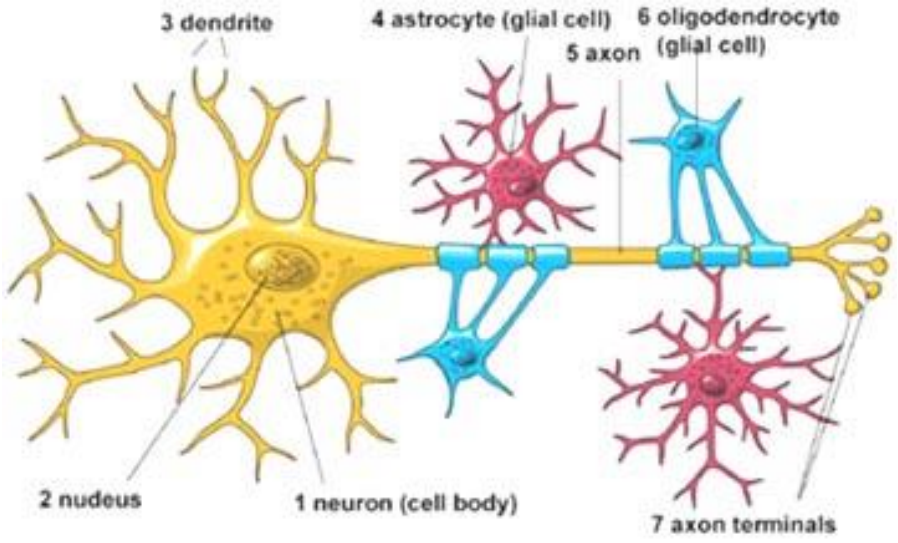


**Figure 1:** The cells of the central nervous system. Neurons (1) conduct electrical activity and are insulated by oligodendrocytes (6). Astrocytes (4) surround the neurons and support them. (Picture source NIH Neurological Disorders and Stroke[16])

Humans begin life with a primitive embryonic nervous system that consists of a tube of neural ectoderm that provides the basis for a central nervous system[17]. Embryonic stem cells develop into neural stem/progenitor cells (NS/PCs) and from there into mature glial and neuronal cells. Although there are many more NS/PCs in a newly forming central nervous system (CNS), it has been shown that there are also stem-like cells within the adult CNS. This is evidenced by the formation of the glial scar following an adult spinal cord injury (SCI)[18]. This response is generated mostly be newly differentiated astrocytes emanating from ependymal cells. The occurrence of a glial scar insinuates that the adult CNS contains NS/PCs that could potentially be employed for therapeutic repair if provided with optimal environmental conditions.

## 1.2 *In vitro* NS/PC Culturing

*In vitro* cell culturing has occurred since 1885 when Wilhelm Roux first maintained extracted chicken cells in warm saline solution on a 2D polystyrene dish[5]. Although sustaining cells in 2D has been beneficial to science over the past century and a half, technological advances of the late 1900's have provided the opportunity to start culturing cells in a more biomimetic environment, e.g. electrospinning organic chemicals[6,7]. Over the past half century hydrogels have emerged as a remarkable platform for culturing cells in 3D with highly tunable and controllable characteristics[8]. This creates the opportunity for 3D *in vitro* microenvironments that can be adapted for specific cell types, such as NS/PCs. NS/PCs represent a multipotent group of cells capable of differentiating into neurons, astrocytes and oligodendrocytes (Figure 2). It has been shown that the mechanical properties and chemical concentration of 3D

microenvironments can affect the survival, proliferation and differentiation pathway of NS/PCs[10].

This research assessed the viability, proliferation and differentiation of GIBCO® Human Neural Stem Cells (H9-Derived). These cells were derived from NIH approved H9 human embryonic cells (hESCs). They were characterized by GIBCO® to show they stained positive for SOX2, Nestin and Ki67 (Table 1). It is important to note that these are human cells because it diverges from previous research of microenvironmental impacts on rodent NS/PCs which behave differently[19].

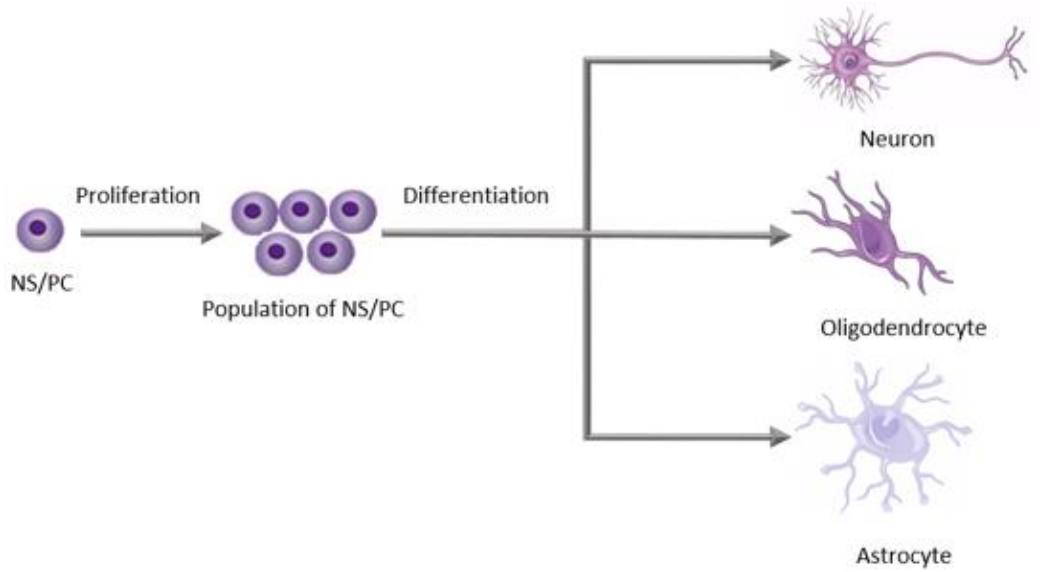


**Figure 2:** Starting with a small population of NS/PCs (left), environmental conditions will determine the amount of proliferation into larger populations of NS/PCs. By modifying the environment, differentiation can be initiated in which NS/PCs will move toward a specific cell fate (Neuron, Oligodendrocyte or Astrocyte).

## CHAPTER 2: HYALURONIC ACID-BASED HYDROGELS

As an approach to therapeutic CNS repair techniques, this research focused on exploring responses of human NS/PCs to their *in vitro* microenvironment. Hyaluronic acid (HA) is a repeating dimer polysaccharide chain composed of N-acetyl-D-Glucosamine and Glucuronic Acid (Figure 3). HA was named by Karl Meyer and John Palmer in 1934, upon their discovery of the polysaccharide within the vitreous body of a cow's eye, after the Greek word "Hyalos", meaning glass, and "uronic", as in the sugar that comprises it[8]. HA falls within the family of glycosaminoglycans because of its linear unbranched polymer structure of repeated disaccharides. However, it is unique within this family in that it is nonsulfated and can branch repeatedly to create very high molecular weight chains[20]. This property is advantageous when considering the chemical as a tool for endogenous CNS repair because it provides unique molecular weight proportions that allows it to expand in areas of high pressure to create avenues for the flow of cells or other particles. This can be observed within the neural crest where NS/PCs begin their migratory pathways before differentiating into specific cell fates[21].

HA is also naturally abundant within most living organisms, as a major component of the extracellular matrix (ECM). HA is also conserved throughout the evolutionary tree underlying its importance in fundamental biology. In such, HA is very biocompatible and most cells in the body have the capability to synthesize and degrade it as necessary[22]. HA has also been shown in high molecular weight form to disrupt the glial scar formation mentioned earlier, while low molecular weight form has shown angiogenic properties that can also be advantageous for SCI repair[23].

Another advantage of HA is that is can be modified through acrylation and thiolation to add binding sites for cross-linking chemicals. Thiolation of HA is particularly advantageous because attaching sulfhydryl bonds to the glucuronic acid monomer (Figure 3) allows the HA chain to not only bind to itself, but also to maleimide terminated crosslinking chemicals, such as four-arm poly-ethylene glycol (PEG)[24]. This allows for the creation of tunable hydrogel scaffolds with many potential chemical structures that result in varied stiffness and structural properties. The cross-linking ability was explored within this research as batches of HA were thiolated to produce HA-thiol (HA-SH) within a range of 4.4-8.5% of glucuronic acid groups thiolated. NS/PCs are commonly found in niches within organisms where HA has been implicated to have an important role in promoting the proliferation and differentiation of cells[25]. Another attribute of using HA-based hydrogels as an *in vitro* NS/PC culturing environment is that the encapsulated gels can subsequently be used as a vehicle for cell delivery to a SCI site. HA has shear thinning properties, meaning that its normal high viscosity decreases in the presence of shear strain[26]. This is an important consideration since a main drawback of cell injections are the death of cells due to shear strain during administration[27].

The second main component of the HA-based hydrogels is PEG, a hydrophilic polyether compound widely used in biological research because of its flexibility and water solubility[28]. It is another highly biocompatible compound and can facilitate cell fusion[29]. A four-arm structure version of the molecule, as used here, can be terminated with thiol groups or maleimides (Figure 4). PEG can also be linked to a variety of peptides, such as RGD. In this research, four-arm PEG-thiol (PEG-SH) was utilized as an additional thiol additive to increase the crosslinks within the hydrogel while maintaining the HA concentration. PEG-maleimide (PEG-Mal) was utilized as a carrier for RGD, a sequence that enables integrin-mediated NS/PC adhesion, and as a cross-

linker that could bind to the thiol chains of the PEG-SH and HA-SH through Michael's Addition chemistry[30].

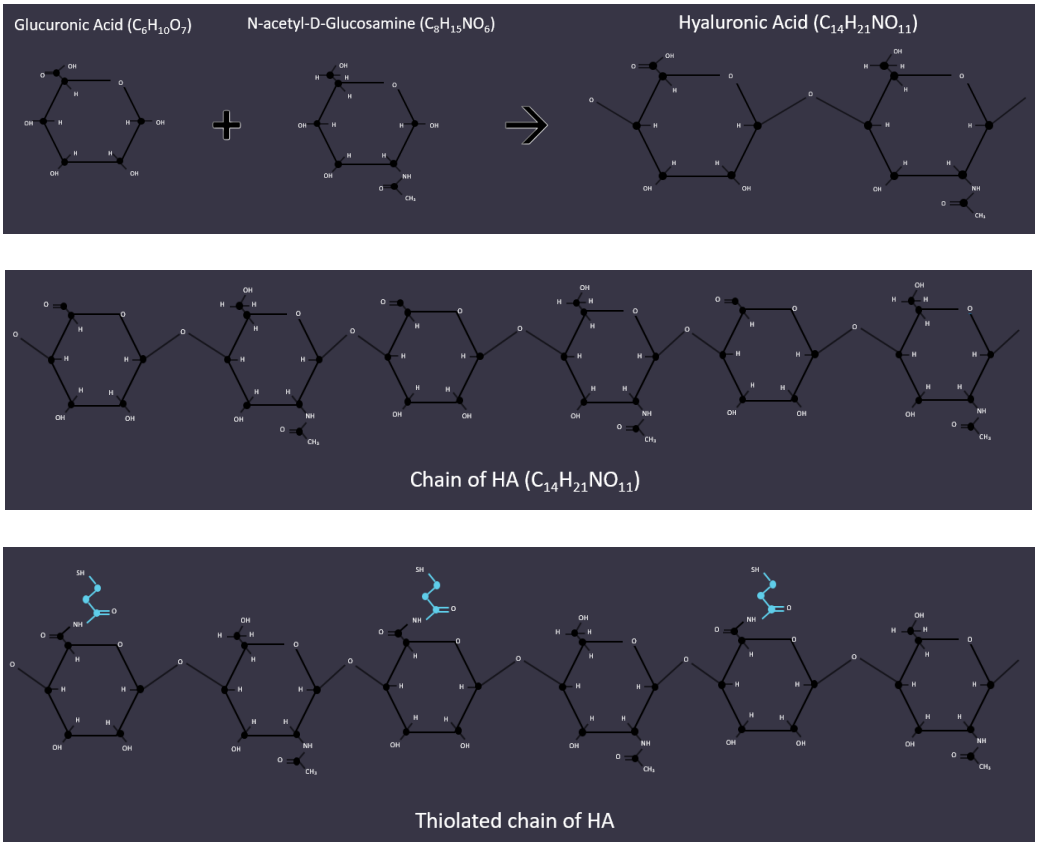


**Figure 3:** Hyaluronic acid (Top) Chain of HA (Middle) and thiolated chain of HA (Bottom)

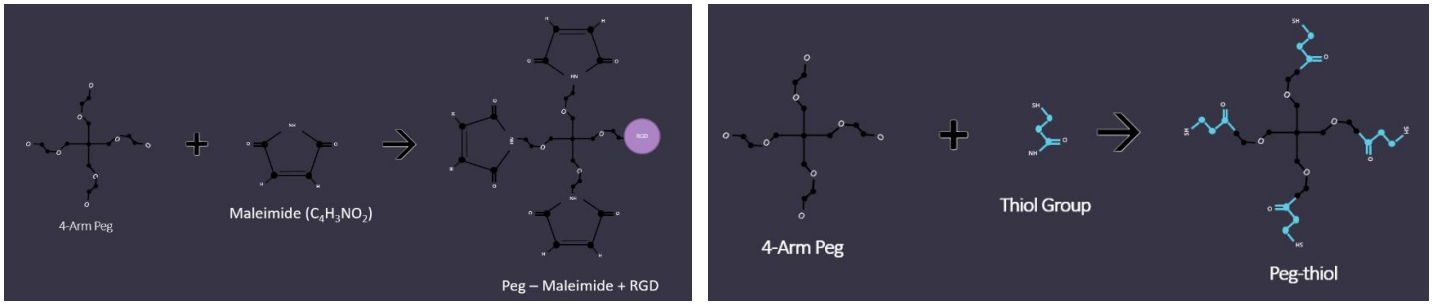


**Figure 4:** (Left) Four-arm polyethylene glycol (PEG) terminated on three arms with maleimide and the fourth by the peptide RGD (PEG-Mal + RGD). (Right) four-arm PEG terminated on all arms by a thiol group (PEG-SH).

# CHAPTER 3: MOTIVATION AND CONTRIBUTIONS

According to the National Spinal Cord Injury Statistical Center 17,700 new SCI cases occur every year in the United States[3]. SCI can be defined as an assault to the central nervous system in a way that impacts ascending peripheral nerve information as well as descending motor commands from the brain[31]. Once this wiring is severed an immunogenic response ensues in which astrocytes infiltrate the injury site and release proteoglycans such as keratin and chondroitin that promote a cascade of effects that can inhibit endogenous repair of the ECM[32]. Because of these combined acute and chronic biological responses to SCI and the fact that there are currently no treatments, nearly all patients are paralyzed for life.

The current prevalence of SCI in the U.S. is about 300,000 people[3]. The average age of injury was 29 in the 1970's, however recent data from 2018 shows this average has increased to a median age of 43. Most SCI cases involve males. The most common cause of SCI are vehicle crashes, followed by falls, acts of violence (gunshot wounds) and sports activities. The first year of costs for the tetraplegic category of injury is $1.1M followed by each subsequent year cost of $191,436. This relates to a total lifetime cost of $4.89M if injured at age 25 and $2.68M if injured at age 50[3].

About one third of persons with SCI are employed twenty years after injury leaving the vast burden of medical care to be paid by taxpayers and insurance companies[3]. Immediately following an injury, the person is immobilized and maintained in the emergency room, sometimes undergoing surgery, spinal alignment techniques and steroid administration to reduce nerve damage and decrease inflammation[33]. Long-term therapy includes physical and occupational rehabilitation sometimes combined with functional electrical stimulation. Typically,

the patient is taught to interact with adaptive mechanisms to regain independence, whether it be a wheelchair or to the extent of an adaptive device for communication purposes[34]. Even with these efforts, the person is living with a limited version of their prior independence and this often leads to depression and an overall decrease in quality of life[35].

### 3.1 Hypotheses and Summary of Results:

This research was guided with the following question in mind: How do mechanical properties (stiffness) and HA content of a 3D microenvironment affect survival, proliferation and differentiation of human NS/PCs? I hypothesized that the proliferation of NS/PCs would increase as stiffness increased, which was proven correct through assessments using two assays, CellTiter-Glo® Luminescent Cell Viability to assess total ATP activity and a DNeasy Blood and Tissue Kit to assess total DNA content 1 and 7 days (D1 and D7) after encapsulation. I also hypothesized that proliferation would decrease as the HA concentration increased, which was true in the soft and medium stiffness gel conditions evaluated. These assumptions were based on empirical evidence as follows. It is well known that CD44, a cell surface receptor present on NS/PCs and astrocytes, interacts with HA to regulate cell proliferation. Mice lacking CD44 show increased NS/PC proliferation, indicating that the presence of CD44 on cells and HA within their environment leads them to a quiescent state in which they are less proliferative[36]. In terms of the effects of microenvironmental stiffness on human NS/PC proliferation, it has been reported that stiffnesses greater than 100 Pascal (Pa) result in robust proliferation[37]. Proliferation peaked when cells were cultured in 1–4 kPa stiffness environments, which best resemble the natural stiffness of human spinal cord tissue[38].

For the differentiation studies, I hypothesized that neurons would result from a softer gel and high HA concentration, while astrocytes would result from a stiffer gel and low HA concentration. I also hypothesized that oligodendrocytes would result from low HA concentrations. The following empirical data was referenced when formulating these hypotheses. The compressive moduli of adult rat spinal cords have been recorded to be around 8 kPa[39] (Figure 5), representing the optimal stiffness to obtain differentiation of NS/PCs into astrocytes[40]. NS/PCs were shown to differentiate most towards neuronal cell types in softer gels[41]. Strong HA signal (higher concentration) was found in areas of differentiating neurons within the spinal cord of chicken embryos[42]. It has been confirmed by multiple researchers that NS/PCs tend to differentiate into neurons when surrounded by a softer environment, most like that of the brain, around 500 Pa [41]. One study reported that the presence of high molecular weight HA is correlated with a prohibition of oligodendrocyte progenitor cells (OPCs) from maturing into oligodendrocytes[42].

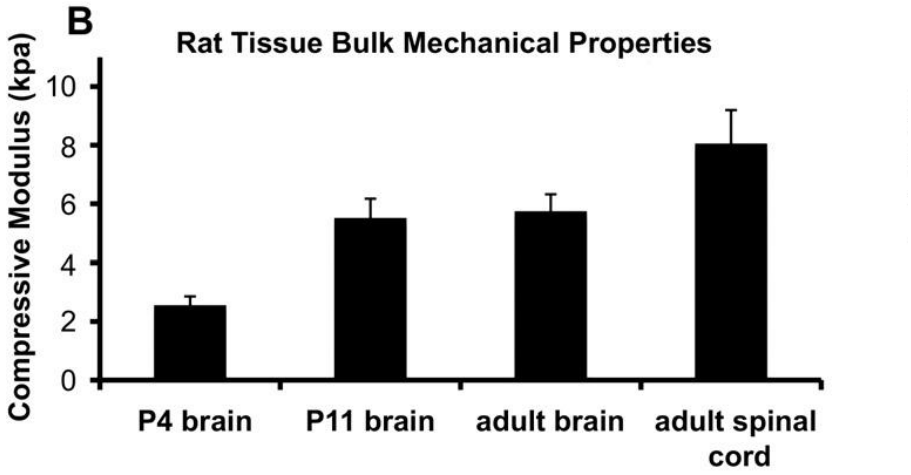


**Figure 5:** This panel represents the bulk mechanical properties of adult rat spinal cord tissue is around 8 kPa (Source Seidlits et al. 2010[39])

**3.2 Experimental Design:**

This research assessed nine different hydrogel conditions plus one control condition, 4B (10 mg/mL HA, 11.6 mg/mL and 150 Pa stiffness), that had parameters matching previous studies from Seidlits lab. The parameters for each gel condition are shown in Table 1 where the rows reference stiffness and the columns reference HA molecular weight percentage. 2D controls were also compared. All conditions were seeded with 100k cells as described in methods section 3.3.3.

The stiffness values (200, 400 and 800 Pa) were chosen because they closely match biological stiffness measurements of human brain tissue and spinal cord respectively. These values had also not been previously tested as an *in vitro* microenvironment for human NS/PC culture providing the opportunity to contribute to the scientific community by filling in some gaps in the research. Finally, these stiffnesses provided enough of a range to observe noticeable differences between the hydrogel conditions in terms of mechanical characteristics and the responses of NS/PCs. The HA weight percentages (0.1%, 0.5% and 1%) were chosen based on empirical evidence of HA concentration values within the spinal cord of different organisms. The 0.1% HA group was included as a hydrogel condition with relatively no HA, while the 0.5% and 1% HA conditions were assessed as biologically relevant HA concentrations.

Figure 6 outlines the timeline of the experiments. There was a total of eight encapsulations performed, two to gain proficiency, three for the proliferation study and three for the differentiation study. Three weeks before encapsulation, the HA was thiolated and tested for thiolation percentage, as explained in the methods section. Two weeks before encapsulation the rheological characterization studies were performed to determine the necessary chemical concentrations of PEG-Mal and PEG-SH for each of the nine conditions since this was directly

related to the measured stiffness and varied between batches of HA-SH. On day zero the encapsulation was performed and on either day 7 (proliferation study) or day 14 (differentiation study) hydrogels were fixed for immunostaining or underwent quantitative assessment. Fixed hydrogels were subsequently sectioned and/or stained starting on day 18 and were imaged on day 28.

| Concentration → <br> Stiffness ↓ | Low | Medium | High |
|---|---|---|---|
| Soft | **1A** <br> 0.1% HA <br> 200 Pascal | **1B** <br> .5% HA <br> 200 Pascal | **1C** <br> 1% <br> 200 Pascal |
| Medium | **2A** <br> 0.1% HA <br> 400 Pascal | **2B** <br> .5% HA <br> 400 Pascal | **2C** <br> 1% <br> 400 Pascal |
| Stiff | **3A** <br> 0.1% HA <br> 800 Pascal | **3B** <br> .5% HA <br> 800 Pascal | **3C** <br> 1% <br> 800 Pascal |

**Table 1:** Ten HA-based hydrogel conditions were compared: **1A**: 200 Pa 0.1 wt% HA, **2A:** 400 Pa 0.1 wt% HA, **3A:** 800 Pa 0.1 wt% HA, **1B:** 200 Pa 0.5 wt% HA, **2B:** 400 Pa 0.5 wt% HA, **3B:** 800 Pa 0.5 wt% HA, **4B Control:** 150 Pa 0.5 wt% HA, **1C:** 200 Pa 1 wt% HA, **2C:** 400 Pa 1 wt% HA, **3C:** 800 Pa 1 wt% HA

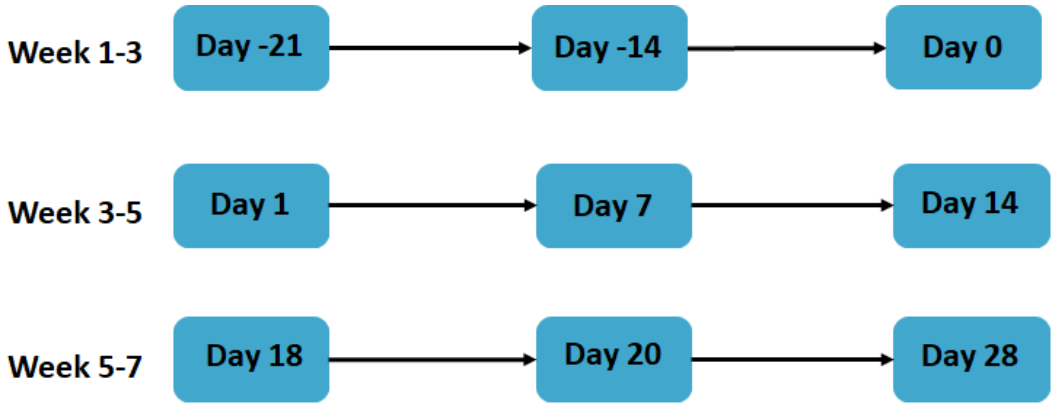


**Figure 6:** Experimental timeline. **D-21:** Start HA thiolation. **D-14:** Begin rheological characterization studies. **D0:** NS/PC Encapsulation. **D1:** CellTiter-Glo® and DNA Assay. **D7:** CellTiter-Glo®, DNA Assay, and fix hydrogels for immunostaining or transition to differentiation media. **D14:** Extract RNA for qPCR, fix and embed hydrogels for immunostaining. **D18:** Section hydrogels. **D20:** Begin staining of hydrogels. **D28:** Image stained sections (Leica SP-2 fluorescent microscope), whole hydrogels (Leica SP-5 confocal microscope) and run qPCR

### 3.3 Methods:

#### 3.3.1 Thiolation of HA

HA (700 kDa, LifeCore Biomedical) was modified in batches to produce a range of 4.4-8.5% thiolation in which thiol groups were added via carboxylic acid of the glucuronic acid molecule within HA through EDC-NHS chemistry (Figure 7). Proton nuclear magnetic resonance (NMR) spectroscopy and an Ellman's test, according to Gold Biotechnology Ellman's Test Protocol,[43] was then used to obtain an idea of the percent thiolation for each batch of HA-SH[44].

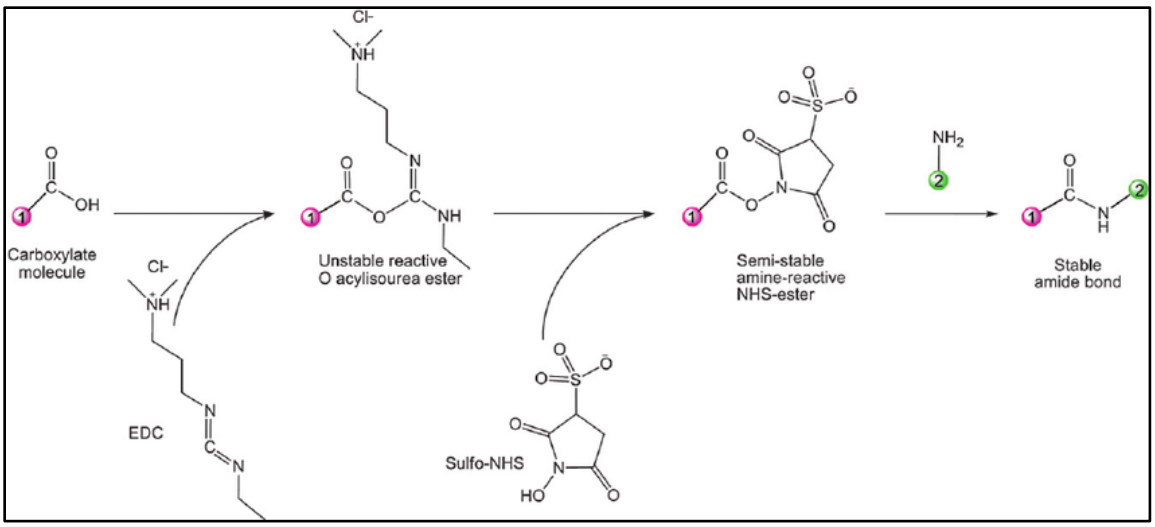


**Figure 7:** Example of EDC-NHS chemistry which was used to add a thiol group to HA (Image source Bart et al. 2014[45])

**Proton** N**MR**

NMR is a measurable phenomenon in which nuclei absorb and then re-emit electromagnetic radiation within a magnetic field. Since different chains of a base molecule respond differently in this process, the results can be mapped as peaks on a curve using Proton NMR. HA-SH (2–5 mg) was weighed and placed in a brown vial to which 1 mL of deuterated water was added along with a magnetic stir bar and set to dissolve on a magnetic stir plate. The entire 1 mL of solution was then added to a glass test vial and brought to the UCLA Molecular Instrument Core Facility for testing.

**Ellman's Test**

Ellman's reagent was also used to quantify the concentration of thiol groups within a sample of each batch of HA-SH (Figure 8).

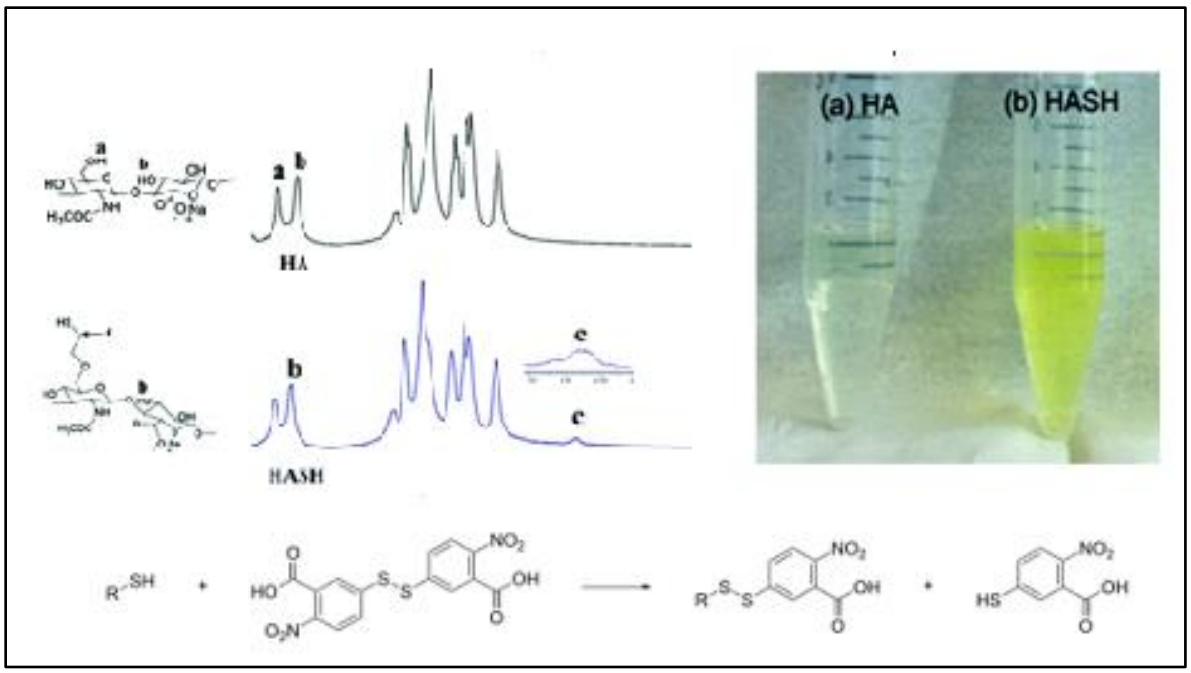


**Figure 8:** Example of Proton NMR results comparing HA and HA-SH (Left), example of Elman's test (Right) and chemical formulation for Ellman's Test (Bottom) (Source Lim Et al. 2016[48])

### 3.3.2 Mechanical Studies of Hydrogels

Since one of the independent parameters of this study was the mechanical properties of the HA-based hydrogels (soft, medium vs. stiff), it was necessary to first characterize the viscoelastic properties of each hydrogel condition. Equation 1 was used to calculate the concentrations of PEG-Mal and PEG-SH for each condition. Starting parameters included the thiolation percentage of the HA-SH and the desired HA weight percentage.

**Equation 1**

Total thiol (mmol) - $\left(\frac{HA\ Concentration}{402\frac{g}{mol}}\right)(percent\ thiolation)$(5000 g/mol) = Total PEG-SH

Total thiol (mmol) / (1.2) = Total PEG-Mal

## Hydrogel Fabrication

Silicone rubber molds (80 µL volume) were first autoclaved, then cooled, dried and placed into the bottom of 24-well plates. Stock solutions of 100 mg/mL 20 kDa 4-arm PEG-Mal (Laysan Bio, Inc), 150 mg/mL 20 kDa 4-arm PEG-SH (Laysan Bio, Inc) and 4 mM cysteine (Sigma-Aldrich) were prepared. HA-SH was placed in a brown vial, weighed, covered with aluminum foil and labeled. A small magnetic stir bar was added as well as HEPES buffer (20 mM, pH 9.0) at three starting concentrations (5 mg/ml, 15 mg/ml and 25 mg/ml). The vial was then placed on a magnetic stir plate and left to dissolve. Meanwhile, the cross-linker solutions (PEG-Mal, Cysteine and PBS) were prepared so that cysteine was conjugated to about 12.5% of maleimide groups of the PEG-Mal. This cross-linker solution was then left for 30 minutes at room temperature.

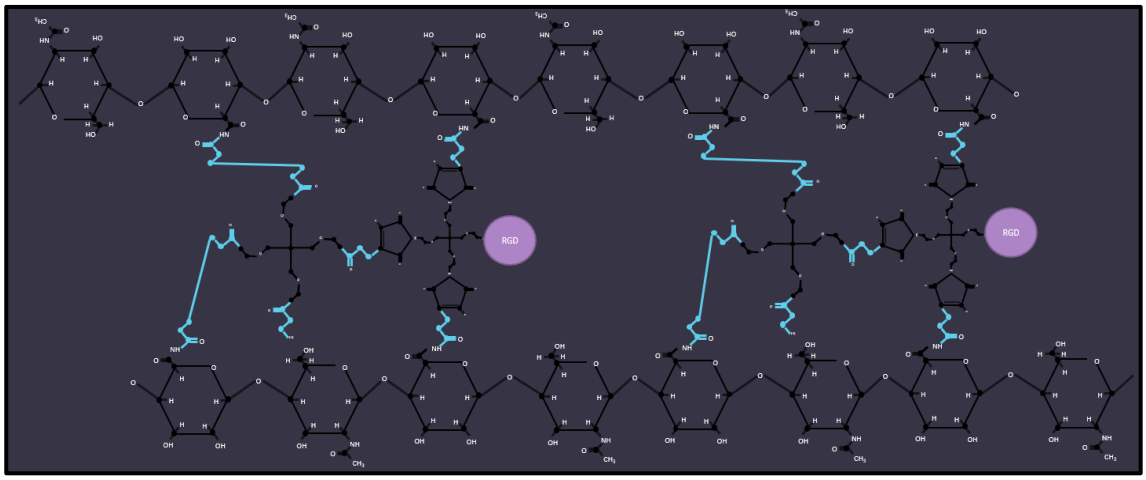


**Figure 9:** An example of a cross-linked matrix formed by the PEG-Mal, PEG-SH and thiolated HA chain (HA-SH). Without molecular level examination this can only be represented as an example of the supposed architecture. Disulfide bonds likely form between thiolated HA dimers as well as between HA-SH and PEG-SH, while thiol-Michael Addiction click reactions create the bonds between HA-SH/PEG-SH and PEG-Mal.

After the HA-SH solutions dissolved they were transferred to 2 mL microcentrifuge tubes and diluted to concentrations of (2 mg/mL, 10 mg/mL and 20 mg/mL). This dilution was accomplished using PEG-SH and Phosphate-Buffered Saline (PBS) to create the pre-calculated solution. This mixture was then pH adjusted to a biological pH (7-7.5) and placed on ice. Next 40 µL of HA-SH solution was added to each mold with a wide-bore pipette tip. Then 40 µL of the cross-linker solution was added to each mold and the solution was pipetted and stirred quickly. Hydrogels were cross-linked via Michael-type Addition (Figure 9). Each group had a minimum of three gels per condition meaning an average run for rheological testing was 30 gels. The well plate was then placed in a bead bath (37°C) for 30 minutes to allow the hydrogels to fully form. The silicone rubber molds were then carefully removed, leaving the hydrogels within the wells. PBS (1 mL) was added to each well, then the well plate was wrapped with Parafilm and stored at 4°C overnight.

**Rheological Characterization of Hydrogels**

Before rheology, a reference gel was fabricated to match the size specifications of the HA-based hydrogels (9 mm diameter x 4 mm height cylinder) according to the following procedure. Polydimethylsiloxane (PDMS) precursors were purchased (Sylgard 184 silicone Elastomer Kit) and combined at a 10:1 ratio of elastomer to curing agent. The mixture was then mixed well, vacuumed to remove all bubbles, added to the same silicone rubber molds used for hydrogel fabrication and placed in an oven at 100°C for 45 minutes. After baking, the PDMS was removed from the silicone molds and stored for rheological testing. This reference PDMS gel was included in the study to serve as a standard that was tested on the rheometer prior to each batch of rheological characterization of the hydrogels.

The day after hydrogel fabrication, the well plate of hydrogels and reference PDMS gel were brought to the Laboratory for the Chemistry of Construction Materials (Boelter Hall) for testing. A Discovery Hybrid Rheometer (TA Instruments HR-2) was fitted with a crosshatched bottom plate maintained at 37°C and a 9 mm parallel plate. The machine was then calibrated and the reference PDMS gel was tested as a standard for the accuracy of the machinery. A frequency sweep of 0.1% - 1% stress/strain was applied to the reference gel and HA-based hydrogel conditions up until 10 Hz. The complex modulus was computed (Equation 2) and these values were saved and averaged for each hydrogel condition. This information was compiled and plotted for each rheological test and total amount thiol was then modified in the hydrogel calculation spreadsheet for the second rheological characterization study. Two independent repeats of hydrogel fabrication were conducted for rheological testing to confirm the target stiffness for each condition since this varied from batch to batch of HA-SH depending on the thiolation percentage.

**Equation 2**

$$\text{Complex Modulus} = \sqrt{(\boldsymbol{G''})^2+(\boldsymbol{G'})^2}$$

### 3.3.3 NS/PC Culture

NS/PCs, GIBCO® Human Neural Stem Cells (H9-Derived), were purchased from Life Technologies, expanded and frozen down at passage three. After thawing and seeding into a T75 flask, they were used for the experiments from passage 3 to 7. After the first week of expansion, they were passaged into three T75 flasks. They were then again passaged during the encapsulation to collect cells for seeding three new T75 flasks, a T25 flask, well plates,

coverglass and hydrogels as described below. The cells were maintained in proliferation media and housed in an incubator between passages (37 °C 5% $CO_2$ 95% humidity). Passaging into flasks and well plates was achieved by pre-coating the flask/well plates with 100:1 Dulbecco's Phosphate-Buffered Saline (DPBS) with Calcium and Magnesium (Genesee Scientific 25-508C) and CTS™ CELLstart™ Substrate (Life Technologies A10142-01). Coverglass were prepared for NS/PC seeding separately. They were first added to a polypropylene holder, cleaned with sulfuric acid, and rinsed with Deionized $H_2O$ until pH of the rinsed water was within the range of 6.5-7. They were then autoclaved and moved to a 24-well plate within the Biosafety Cabinet (BSC). Next the coverglass was coated with 50 µg/mL poly-D-lysine hydrobromide 30,000 - 70,000 molecular weight (Sigma-Aldrich P7886) in sterile, distilled and deionized $H_2O$ and placed in a 37°C incubator for about one hour. Next, they were rinsed with DPBS -Ca/-Mg (Thermo Fisher 14190250) and then incubated with 10 µg/mL Laminin, Mouse (Corning™ 354232) in sterile distilled $H_2O$ in an incubator (37 °C 5% $CO_2$ 95% humidity) overnight. Cells were seeded into flasks at 13,333 cells/$cm^2$ meaning about 2.1 million cells per T75 and about 330,000 cells per T25. After coating, coverglass (113 $cm^2$) were moved to a 24-well plate and along with wells of the coated 24-well plates (1.9 $cm^2$) were seeded with 100,000 cells to remain consistent with the number of cells seeded within hydrogels. Coverglass started with about 8,000 cells/$cm^2$ and the well plates with about 52,000 cells/$cm^2$. Medium was changed every other day and cells were passaged every seven days or at around 90% confluency.

When passaging, all medium was removed from the flask and 5 mL of TrypLE Express (Life Technologies 12604013) were added. The flask was then placed in an incubator (37 °C 5% $CO_2$ 95% humidity) for 2-3 minutes. Then, 10 mL of media were added to the flasks to stop the reaction and cells were visibly seen floating. Next, the flask contents were transferred to a 15 mL

conical tube and spun in a centrifuge according to these parameters: 9 acceleration, 7 deceleration, 150 x g for 5 minutes at room temperature. Next, the supernatant was aspirated leaving the pellet of cells behind. This pellet was resuspended in 1 mL of media and combined at a 1:1 or 1:2 ratio with Trypan Blue solution (Sigma-Aldrich T8154) to count viable cells. Next, the appropriate volume of cell solution was added to a pre-coated flask, well plate, coverglass or HA-SH solution.

**NS/PCs in 2D (Control)**

Two forms of 2D controls were used in this study, cells seeded onto well plates and coated coverglass. Some of the well plates were used as a CellTiter-Glo® Luminescent Cell Viability Assay (Promega G7572) control group and some well plates and coverglass were used for immunostaining.

**NS/PCs in 3D (Encapsulation)**

Before encapsulation, solution calculations were determined based on the thiolation percentage of HA, total thiol (mmol) desired, a 1:1.2 molar ratio of total thiol (contributed by PEG-SH and HA-SH) to PEG-Mal and 1:8 ratio of RGD to PEG-Mal. For example, in encapsulation eight for the 1A group (Table 5) the total thiol was controlled to be 0.0025 mmol per 110 µL resulting in a total PEG-Mal of 0.00275 mmol per 110 µL. Silicone rubber molds (20 µL volume) were autoclaved, cooled and placed into plastic Petri dishes. 48-well plates were prepared with proliferation media (500 µl per well). Cross-linker solutions (PEG-Mal, RGD and PBS) were prepared according to the calculations for each condition and the first HA-SH solution was set to dissolve. RGD was used instead of Cysteine for the encapsulations but concentrated in the same manner so it was conjugated to about 12.5% of maleimide groups of the

PEG-Mal. While the HA-SH dissolved, T75 flasks were passaged to prepare cell solutions for the three HA conditions (3.3 – 4.4 million cells) in 15 mL conical tubes. The pellets were then resuspended in 15-25 µL. Once the HA-SH solution was dissolved, it was combined with PEG-SH in PBS to achieve the final HA concentration (0.1 wt%, 0.5 wt% or 1 wt%). The mixture was pH adjusted to approximately 7.4 and 5 µL or 1.1 million cells was added to the HA-SH solution to have a total of 110 µL, enough for ten gels per condition and one extra.

Next, the silicone molds were placed in a Petri dish and 10 µL of the HA-SH solution were added to each mold. Next 10 µL of the cross-linker solution were added and a pipette tip was used to pipette and stir quickly until the gel formed. At this point, the Petri dish was placed in the incubator (37 °C 5% $CO_2$ 95% humidity) for 30 minutes. When the gels were fully formed, they were separated from the silicone molds and carefully transferred to the wells of a 48-well plate that were prepared with media. This was repeated for each of the ten group conditions for 8-10 gels per condition.

**Maintenance Media**

Growth medium was prepared separately for the proliferation and differentiation stages of the experiment. On day seven, encapsulated hydrogels were transitioned to differentiation media.

Proliferation Media: 48.5 mL Knockout Dulbecco's Modified Eagle's Medium F-12 (Genesee Scientific 1260-012), 0.2X Antibiotic-antimycotic (LifeTechnologies 1524XZ0062), 2 mM Glutamax (ThermoFisher 35050061), 20 ng/mL Epidermal Growth Factor (PeproTech AF-100-15), 20 ng/mL Basic Fibroblast Growth Factor (PeproTech 100-18B), and 2% Stempro supplement (LifeTechnologies A1050901)

Differentiation Media: 48.5 mL Knockout Dulbecco's Modified Eagle's Medium F-12 (Genesee Scientific 1260-012), 2% Stempro supplement (LifeTechnologies A1050901), 2% GEM21 supplement (Gemini Bio 400-160), 1 ng/mL Basic Fibroblast Growth Factor (PeproTech 100-18B), 10 ng/mL Brain Derived Neurotrophic Factor (PeproTech 450-02) and Glial cell line-Derived Neurotrophic Factor (PeproTech 450-10), 1% Antibiotic-antimycotic (LifeTechnologies 15240062), 63 µg/mL N-acetylcysteine (Sigma-Aldrich A7250-10G) and 2 µg/mL Heparin (Sigma-Aldrich H3149). Adapted from the formulation used in Nguyen et al.[46]

### 3.3.4 Qualitative Assessment

Immunostaining was performed on well plates, coverglass, cryosectioned hydrogels and whole hydrogels on day 7 (Proliferation) and day 14 (Differentiation). Immunostaining for cParp, Live/Dead, SOX2 and Ki67 was performed to assess overall viability, stemness and proliferation of NS/PCs (Table 2). For the differentiation study, GFAP (astrocytes), DCX (neuron) and PDGFRα (oligodendrocytes) were immunostained for to identify the presence of specific neural cell fates (Table 2).

| Target | Definition | Stage of Experiment |
|---|---|---|
| **Nestin** | A type of intermediate filament protein, expressed in radially growing axons. | Characterization By Gibco® Technologies |
| **Oct-4** | A homeodomain transcription factor that has been implicated in the self-renewal of embryonic stem cells. | Characterization By Gibco® Technologies |
| **Hoescht** | Identifies cell nuclei | All |
| **cParp** | Cleaved PARP. When PARP-1 is broken apart it cleaves into different size molecular weight fragments. This antibody recognizes the 85 kDA fragment of cleaved PARP-1 and can be used as a marker for detecting apoptotic cells. PARP-1 is a preferred substrate of proteases that lead to apoptosis. | Viability |
| **Live/Dead** | Green-fluorescent calcein-AM which indicates intracellular esterase activity. Intracellular esterases are an indication of normal cell functionality and when they come into contact with this dye they will cause it to fluoresce green. Ethidium homodimer-1 which can indicate loss of plasma membrane integrity. This molecule has high-affinity for nucleic acid and weakly fluoresces until bound to DNA. | Viability |
| **Ki67** | Cellular marker for proliferation because it is present in the cell nucleus during interphase and on the chromosome surface during mitosis. | Proliferation |
| **Sox2** | A transcription factor that is important for maintaining pluripotency and had been associated with ribosomal RNA synthesis. Also has a role in maintaining neural stem cell characteristics. | Proliferation |
| **PDGFRα** | Platelet derived growth factor alpha. Expressed by glia and some other neural cells within the central nervous system. Can be used as a marker for oligodendrocytes. | Differentiation |
| **DCX** | Doublecortin is a microtubule-associated protein that can be used as a marker for neuronal migration. | Differentiation |
| **GFAP** | Glial fibrillary acidic protein is an intermediate filament protein that can be used as a marker for astrocytes. | Differentiation |

**Table 2:** Immunostaining targets, definitions and experimental stage

## Fixing and Sectioning

On days 7 and 14 (D7 and D14), gels were fixed for 30 minutes with 4% paraformaldehyde. Some hydrogels were then embedded with 20% OCT-sucrose (Tissue-Plus OCT Compound Fisher Scientific 23-730-571) and sectioned the next day in the Translational

Pathology Core Laboratory (TPCL) on their Leica Cryostat. Gels were sliced into 18 µm-thick sections and placed onto positively charged microscope slides.

**Immunostaining**

Hydrogel sections were subsequently immunostained using the following protocol. Sections were outlined with a wax marker, labeled and fixed with 4% paraformaldehyde to the microscope slides. Next, they were rinsed (3 x five minutes) with PBS-Tween (0.05%), permeabilized with PBS-Triton (0.1%) and then rinsed again (3 x five minutes). Blocking solution was prepared, 4% Normal Donkey Serum (Sigma-Aldrich D9663) and 2% Bovine Serum Albumin (Spectrum Chemical 22070008) in PBS-Tween (0.05%) and added to each section of the slide. This was left for an hour at room temperature, then the slides were rinsed again with PBS-Tween (3 x five minutes) and the primary antibody solutions were added (Table 3). Slides were stored overnight at 4°C and the next day the secondary antibody solutions were added (Table 3). Slides were then mounted with coverslips using Fluoromount G (Fisher Scientific OB100-01), dried overnight and the edges were sealed with clear nail polish. Whole hydrogel immunostaining involved the same process as above, however the times for each step were extended threefold and all steps were performed within the 48-well plate. Whole hydrogels were mounted on concavity slides.

Sections were imaged on a Leica SP-2 fluorescent microscope (100x and 200x magnification) while whole hydrogels were imaged in the CNSI Advanced Light Microscopy Lab on an SP-5 Blue confocal microscope (100x magnification Airy 1 pinhole 53.03µm). Whole hydrogel images were composed of 25 z-stacks of 4 µm sections (100 µm stacks) and processed using LAS-X software to reconstruct 3D hydrogel image stacks and videos.

| Target | Primary Antibody | Dilution Factor (1°) | Secondary Antibody | Dilution Factor (2°) |
|---|---|---|---|---|
| **Nestin** | N/A | N/A | N/A | N/A |
| **Oct-4** | N/A | N/A | N/A | N/A |
| **Hoescht** | N/A | N/A | Hoescht 33342, Trihydrochloride, Trihydrate 10 mg/mL Thermo Fisher Scientific H3570 | 1:1000 |
| **cParp** | Rabbit anti-Cleaved PARP monoclonal Cell Signaling Technologies 9661S | 1:400 | Donkey anti-Rabbit IgG (H+L) Secondary Antibody, Alexa Fluor® 555 Thermo Fisher Scientific A-31572 | 1:200 |
| **Live/Dead** | LIVE/DEAD Viability Kit Life Technologies L3224 | Calcein AM: 10 µM EthD-1: 10 µM | N/A | N/A |
| **Ki67** | Mouse anti-Ki67 monoclonal Millipore MAB4190 | 1:200 | Donkey anti-Mouse IgG (H+L) Secondary Antibody, Alexa Fluor® 488 conjugate Thermo Fisher Scientific A-21202 | 1:200 |
| **Sox2** | Rabbit anti-Sox2 polyclonal Abcam AB97969 | 1:200 | Donkey anti-Rabbit IgG (H+L) Secondary Antibody, Alexa Fluor® 555 Thermo Fisher Scientific A-31572 | 1:200 |
| **PDGFRα** | Rabbit anti-PDGFRα polyclonal Sant Cruz Biotechnology SC-338 | 1:100 | Donkey anti-Rabbit IgG (H+L) Secondary Antibody, Alexa Fluor® 555 Thermo Fisher Scientific A-31572 | 1:200 |
| **DCX** | Mouse anti-DCX monoclonal EMD Millipore MABN707 | 1:500 | Donkey anti-Mouse IgG (H+L) Secondary Antibody, Alexa Fluor® 488 conjugate Thermo Fisher Scientific A-21202 | 1:200 |
| **GFAP** | Chicken anti-GFAP polyclonal Aves Labs GFAP | 1:2000 | Goat anti-Chicken IgY (H+L) Secondary Antibody, Alexa Fluor®647 Thermo Fisher Scientific A-21449 | 1:200 |

**Table 3:** Immunostaining primary and secondary antibody dilution factors

### 3.3.5 Quantitative Assessment

CellTiter-Glo® Luminescent Cell Viability Assay (Promega G7572) was used to assess the amount of Adenosine triphosphate (ATP) present in each condition while a DNA Assay quantified the amount of DNA present using the DNeasy Blood and Tissue Kit (Qiagen 69504). Together, these two quantitative assays were used to obtain an overall idea of how the cells

responded to the different microenvironments based on their metabolic activity and total cell number (whether alive or dead).

CellTiter-Glo® Luminescent Cell Viability Assay, was aliquoted before use (stored at -20°C). On day 7 gels were removed from their 48-well plates using a wide-bore 200 uL pipette and two of each condition were combined in a 2 mL microcentrifuge tube. The gels were then broken up using a 20G needle fitted onto a 1 mL syringe. Next, 75 µL of Knockout Dulbecco's Modified Eagle's Medium F-12 was added to each tube to attain a total volume of about 150 µL. An equal volume (150 µL) of CellTiter-Glo® solution was added to each tube, mixed well with a 200 µL pipette and left to sit for two hours. Meanwhile, four wells of a seeded 24-well plate were prepared in the same manner as controls. Each condition had at least two duplicates containing two gels. A T25 flask was also passaged and serial dilutions were prepared to create a standard curve of cell concentration (0 to 100k cells). These standards underwent the same procedure as hydrogel and control groups. After two hours 100 µL of the hydrogel/cell/ CellTiter-Glo® mixture from each condition, controls and standards were pipetted into four wells of an opaque bottom 96-well plate. The 96-well plate was set up according to Figure 10. The plate was then read on a plate reader (BioTek Synergy II) and duplicates were averaged.

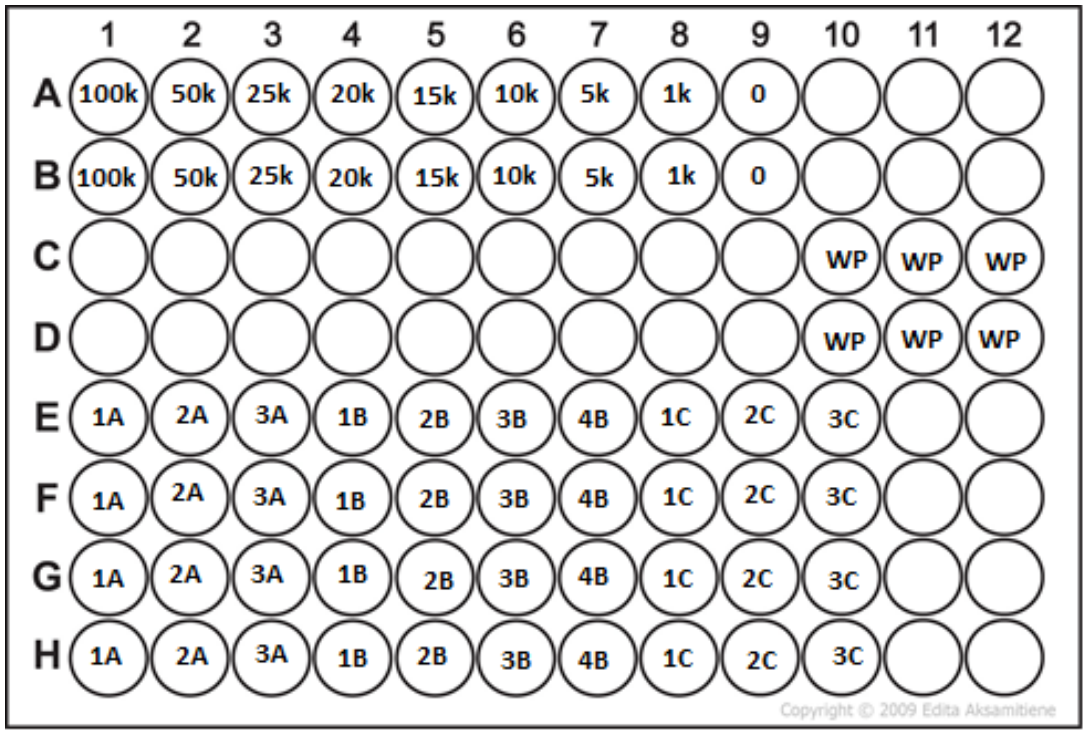


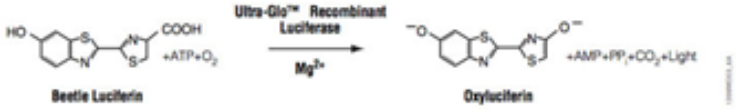


**Figure 10:** Setup of 96-well plate for CellTiter-Glo® (Top) and chemical mechanism of CellTiter-Glo® [48] (Bottom) (Source Promega, Inc). Rows A and B were used for standard solutions of cells ranging from 0 to 100k cells. WP: Well plate.

**DNA Assay**

DNeasy Blood and Tissue Kit (Qiagen 69504) was purchased and a modified procedure was performed as follows. Contents of the 96-well plate that was used to perform CellTiter-Glo® were removed, added to separate 2 mL microcentrifuge tubes and spun for 5 minutes at 300 x g. The supernatant was aspirated and 200 µL of PBS, 20 µL of Proteinase K and 200 µl of Buffer AL were added. The tubes were vortexed and incubated at 56° C for 10 minutes. Next, 200 µl of

100% ethanol was added and the tubes were vortexed. The total volume was then transferred to a DNeasy mini spin column within a collection tube and spun for 1 minute at 6000 x g. The spin column was moved to a new collection tube, 500 µl of Buffer AW1 was added and then centrifuged for 1 minute at 6000 x g. This step was then repeated with Buffer AW2 but centrifuged for 3 minutes at 20,000 x g. The spin column was then transferred to a new 2 mL tube and the DNA was eluted with 40 µl of Buffer AE and incubated for 5 minutes at 37°C. The tube was centrifuged for 1 minute at 6000 x g and this step was repeated a second time. After blanking with Buffer AE, each sample was read on a NanoDropTM 2000/2000c Spectrophotometer.

**RNA extraction**

Using the QuantiTect Probe RT-PCR Kit (Qiagen 204445), RNA was extracted in the following manner. On Day 14, 6 gels per condition were removed from the 48-well plate and placed in a 2 mL microcentrifuge tube by condition. Gels were then broken up with a 20G needle on a 1 mL syringe. 350 µL of Buffer RLT was added to each tube and the total volume was then added into a QIAshredder and centrifuged at full speed. The supernatant was then transferred to an RNeasy spin column and spun for 5 minutes at 8000 x g. Next, 700 µL of buffer RW1 was added and the column was spun at 10000 x g for 15 seconds. This was then repeated twice with 500 µL RPE buffer and once with no added solution. The spin column was then added to a new collection tube and 30 µl of RNase free water was added and incubated for 5 minutes at 37°C.

The tube was spun a final time for 1 minute at 8000 x g. After blanking with RNase free water, each sample was read on a NanoDropTM 2000/2000c Spectrophotometer. (Figure 11)

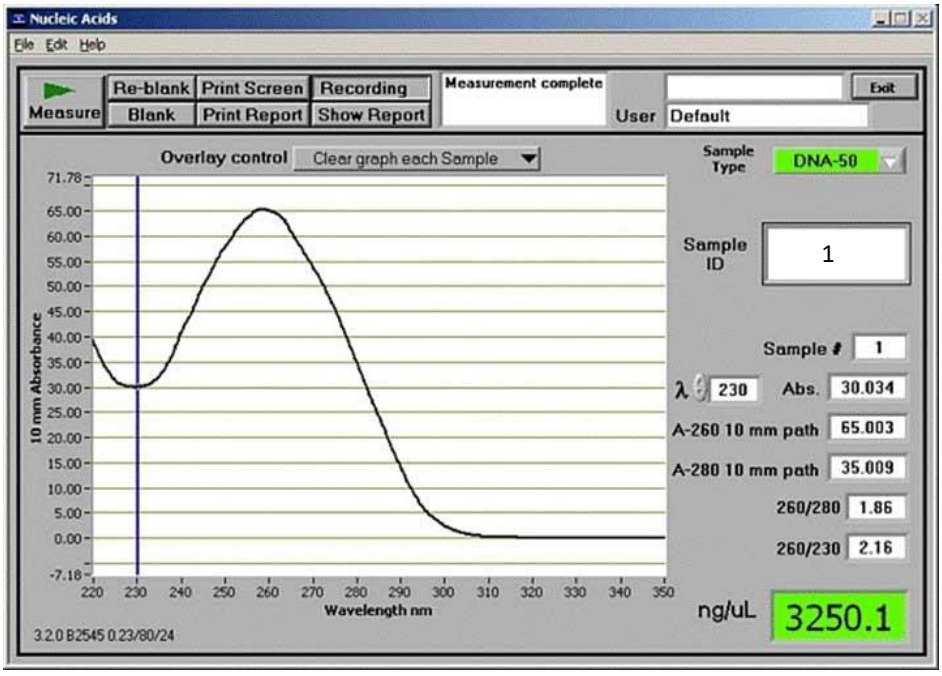


**Figure 11:** Example of reading from spectrophotometer. Notice the peak at 260nm. (Source BYU College of Life Sciences)

**Quantitative Polymerase Chain Reaction (qPCR):**

The RNA was then stored at -80°C until use. The procedure provided by QuantiTect Probe RT-PCR Handbook was followed to prepare a 96-well plate for analysis. A large solution of QuantiTect Probe RT-PCR Master Mix, QuantiTect RT mix, RNase free water were combined and separated into five 2 mL microcentrifuge tubes. Then the five primers were added individually (Table 4). Each primer (47 µL) was loaded into a 96-well plate in duplicate as depicted in Figure 12. RNA was diluted to 10 µg/mL and 3 µL was also added to the appropriate wells. The 96-well plate was then read according to the following real-time cycler conditions: 30 min at 50°C, 15 min at 95°C, 15s at 94°C and 60s at 60°C for 40 cycles.

| Target | Definition | Stage of Experiment | Primer |
|---|---|---|---|
| **MAP2** | Microtubule-protein 2 that can be used as a marker for neurons. Usually localized in dendrite. | Differentiation | Thermo Fisher Scientific Ha00258900_m1 |
| **GFAP** | Glial fibrillary acidic protein is an intermediate filament protein that can be used as a marker for astrocytes. | Differentiation | Thermo Fisher Scientific Hs00909233_m |
| **PDGFRα** | Platelet derived growth factor alpha. Expressed by glia and some other neural cells within the central nervous system. Can be used as a marker for oligodendrocytes. | Differentiation | Thermo Fisher Scientific Hs00258900_m1 |
| **Sox2** | A transcription factor that is important for maintaining pluripotency and has been associated with ribosomal RNA synthesis Also has a role in maintaining neural stem cell characteristics. | Proliferation | Thermo Fisher Scientific Hs01053049_s1 |

**Table 4:** Primers used for qPCR

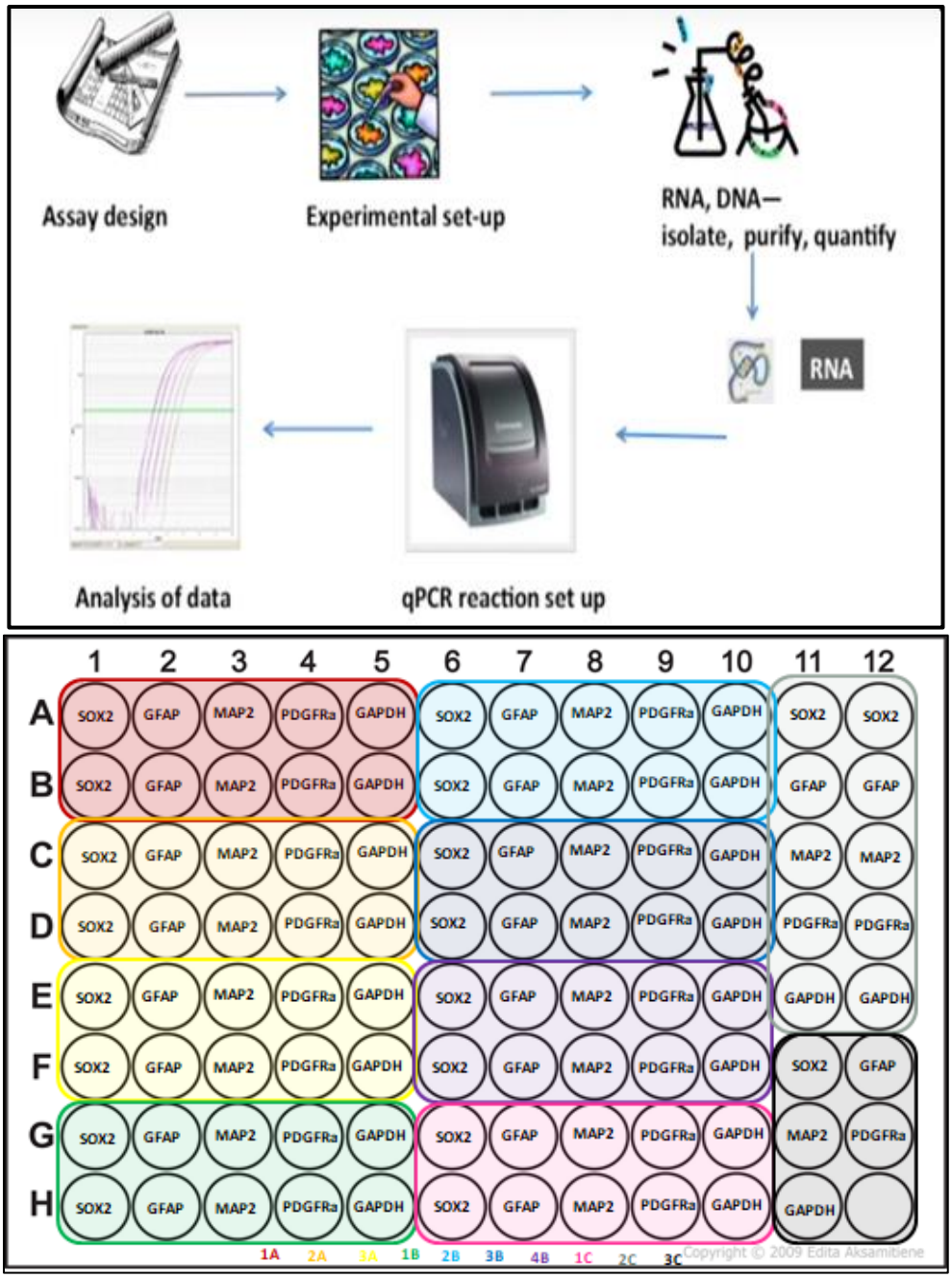


**Figure 12:** General flow of qPCR procedure (Top) (Source Integrated DNA Technologies). Layout of 96-well plate (Bottom)

### 3.4 Results:

#### 3.4.1 Rheological Characterization

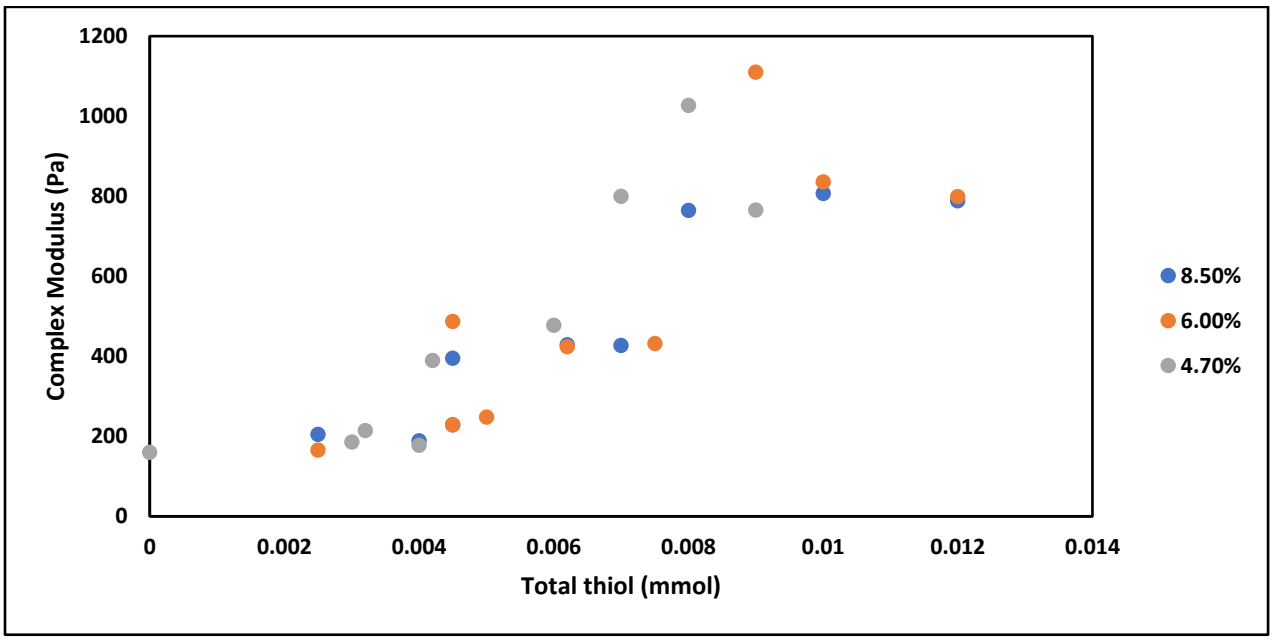


**Figure 13:** Total thiol, contributed by HA-SH and PEG-SH compared to Complex Modulus. Three batches of HA are shown (4.70%, 6.00% and 8.5% thiolation)

Rheological characterization was performed for each independent cell encapsulation experiment (E1-E8). Figure 13 shows three examples of these characterization studies comparing the total thiol within the gels, assuming a 1:1.2 molar ratio of thiol to maleimide, to the complex modulus. The complex modulus was calculated according to Equation 2 which input the storage modulus (G') and loss modulus (G'') read out from the Discovery Hybrid Rheometer (TA Instruments HR-2) Trios software. Variance was seen in the complex moduli even when the same total thiol was maintained for different batches of HA-SH. This represents the need for doing separate rheological characterization for each batch of thiolated HA to confirm the correct stiffness values and adjust the total thiol accordingly. Table 5 shows an example of the

rheological results from an 8.5% thiolation batch of HA-SH. Each stiffness group (200, 400 and 800 Pa) can be achieved for the three HA concentrations (0.1 wt%, 0.5 wt% and 1 wt%).

| Concentration → <br> Stiffness ↓ | Low <br> 0.1% HA | Medium <br> 0.5% HA | High <br> 1% HA |
|---|---|---|---|
| Soft <br> 200 Pascal | **1A** <br> Total Thiol: 0.0025mmol <br> **200 +/- 15 Pascal** | **1B** <br> Total Thiol: 0.0045mmol <br> **230 +/- 80 Pascal** | **1C** <br> Total Thiol: 0.004mmol <br> **190 +/- 20 Pascal** |
| Standard <br> 400 Pascal | **2A** <br> Total Thiol: 0.0045mmol <br> **400 +/- 20 Pascal** | **2B** <br> Total Thiol: 0.0062mmol <br> **430 +/- 20 Pascal** | **2C** <br> Total Thiol: 0.007mmol <br> **430 +/- 30 Pascal** |
| Stiff <br> 800 Pascal | **3A** <br> Total Thiol: 0.008mmol <br> **770 +/- 30 Pascal** | **3B** <br> Total Thiol: 0.01mmol <br> **810 +/- 100 Pascal** | **3C** <br> Total Thiol: 0.012mmol <br> **790 +/- 190 Pascal** |

**Table 5:** Following the experimental design, this table shows complex modulus values for each of the nine conditions tested in this research. **1A**: 200 Pa 0.1 wt% HA, **2A:** 400 Pa 0.1 wt% HA, **3A:** 800 Pa 0.1 wt% HA, **1B:** 200 Pa 0.5 wt% HA, **2B:** 400 Pa 0.5 wt% HA, **3B:** 800 Pa 0.5 wt% HA, **4B Control:** 150 Pa 0.5 wt% HA, **1C:** 200 Pa 1 wt% HA, **2C:** 400 Pa 1 wt% HA, **3C:** 800 Pa 1 wt%. HA-SH percentage thiolation was 8.5% (Encapsulation 2)

### 3.4.2 NS/PC Viability

Viability of NS/PCs within each hydrogel condition was determined qualitatively using immunostaining of cParp and Live/Dead on day 7. Figure 14 demonstrates a 100x view of hydrogel sections (18 µm) and control coverglass. Note that the soft (200 Pa) condition appeared to have more cParp than the medium (400 Pa) and stiff (800 Pa) hydrogel condition. Figure 15 demonstrates a 200x view of the same sections to give a better idea of cell density. Most hydrogel conditions show approximately the same density of NS/PCs, however the medium (400

Pa) and high (800 Pa) stiffness 1 wt % HA conditions had more aggregation of cells. The 2B* group, which was seeded at a density of 200k cells rather than 100k cells, appears to have the largest amount of cell aggregation.

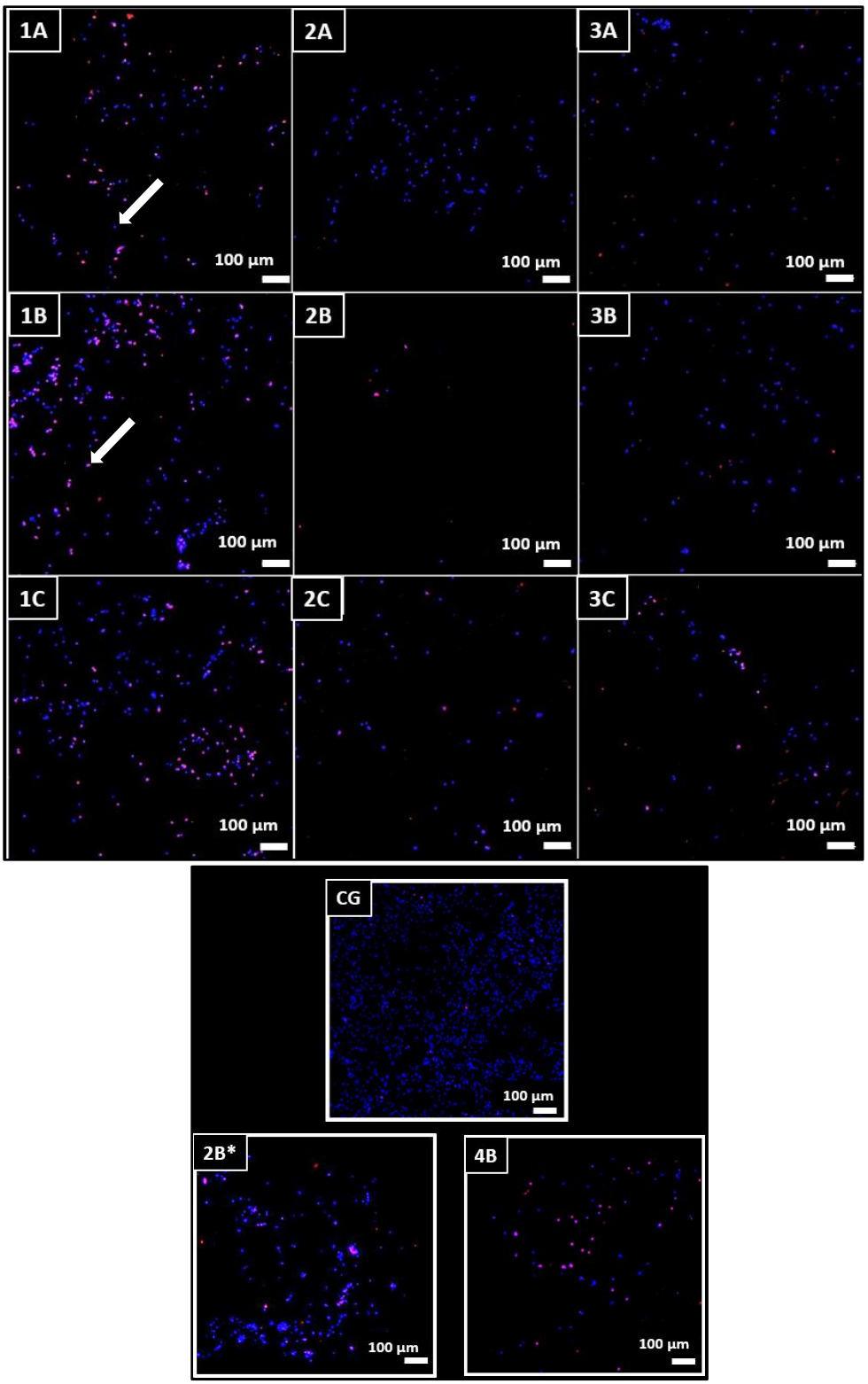


**Figure 14:** Immunostaining for cParp and Hoescht to qualitatively compare the number of apoptotic cells to total number of cells. (Top) Images shown are 18 µm slices of hydrogels sectioned after day 7 onto slides. (Bottom) Controls include coverglass, 4B and 2B* which had

the same formulation as 2B, but was used to compare a seeding density of 200k cells to the otherwise used 100k cells per hydrogel. Top arrow points to a cParp negative cell and bottom arrow to a cParp positive cell. Scale bars are 100 µm.

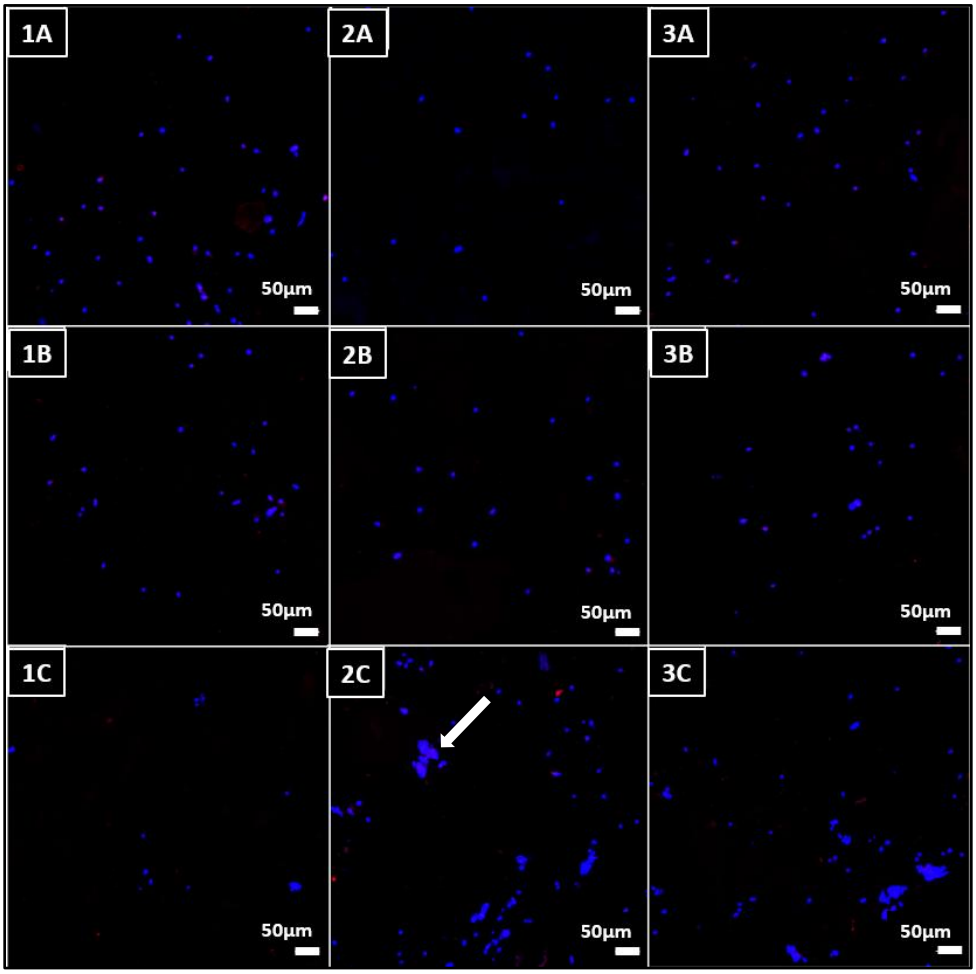


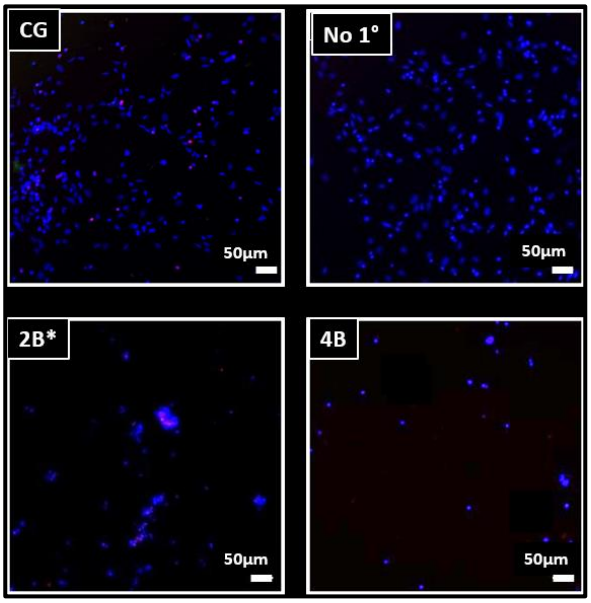

**Figure 15:** Immunostaining for cParp and Hoescht to qualitatively compare the number of apoptotic cells to total number of cells. (Top) Images shown are 18 µm slices of hydrogels sectioned after day 7 onto slides. (Bottom) Controls include coverglass, coverglass with no primary antibodies, 4B and 2B* which had the same formulation as 2B, but was used to compare a seeding density of 200k cells to the otherwise used 100k cells per hydrogel. Arrow points to a group of aggregated cells. Scale bars are 50 µm.

Results shown in Figure 16 are from whole hydrogel staining and thus give a better representation of the overall viability within the hydrogels in that they are more representative of the NS/PC population of the entire hydrogel compared to an 18 µm section. However, since they were imaged using a widefield fluorescent microscope there is some blurriness in the images. These qualitative results show that the highest populations of NS/PCs were seen within the 0.1 wt% HA condition and 0.5 wt% HA condition hydrogels as compared to the 1 wt% HA hydrogels. There are many more dead cells seen in the 1 wt% HA conditions in general as well as the stiff (800 Pa) 0.5 wt% HA condition and medium (400 Pa) 0.1 wt% HA condition.

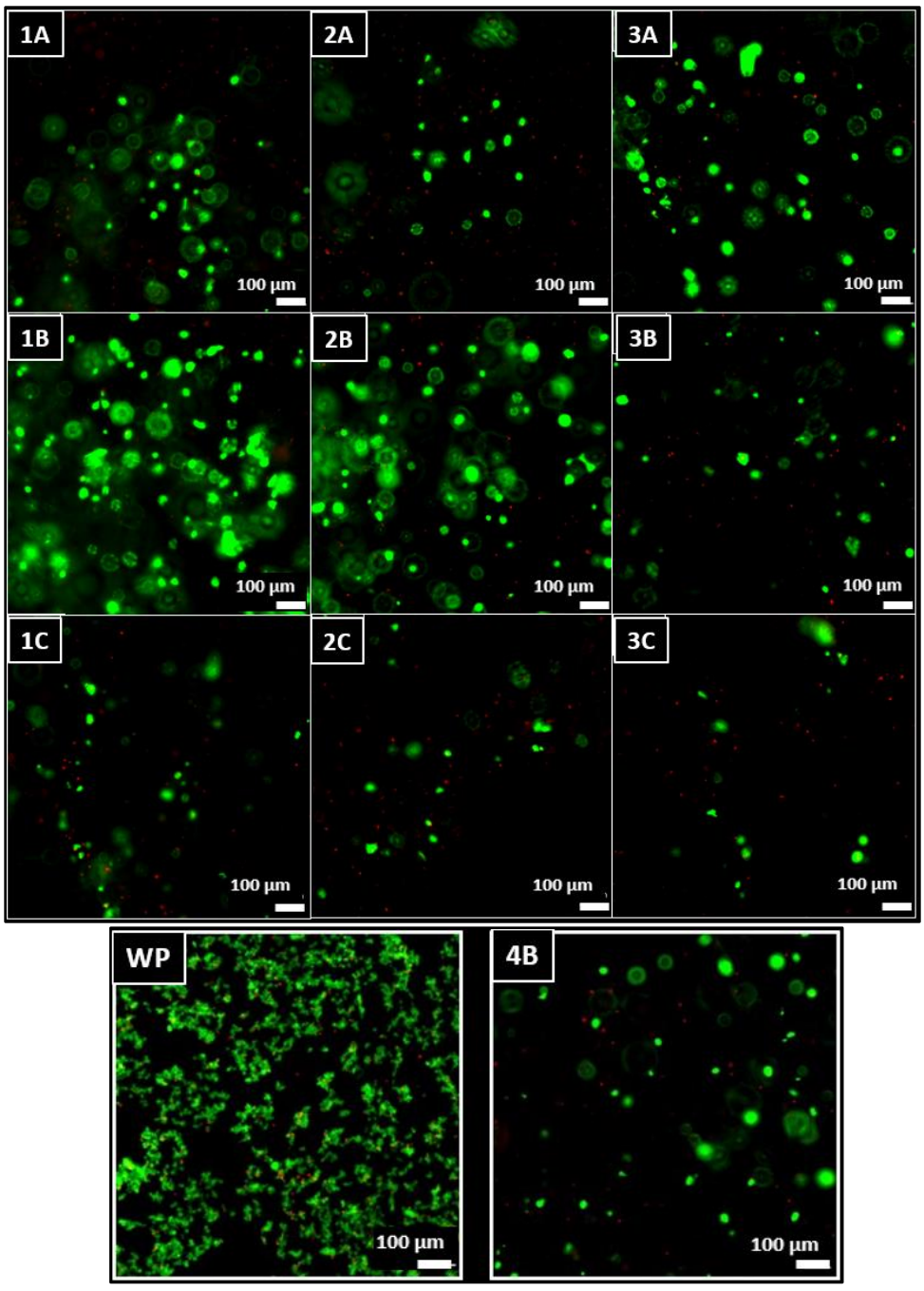


**Figure 16:** Immunostaining of Live/Dead (Calcein-Am/Ethidium homodimer-1) to assess amount of dead vs. live cells. (Top) Images shown are 100x magnification through whole hydrogels. (Bottom) Controls include a well plate and whole hydrogel 4B. Scale bars are 100 µm.

### 3.4.3 Proliferation

Luminescence values from the standard solutions read during CellTiter-Glo® were used to plot a standard curve on days 1 and 7 (Figure 17) to relate luminescent readings to cell number. An assumption was made that the average ATP within one cell would be equal between cells cultured in the T25 flask and those within the hydrogels. These quantitative results represent the amount of ATP present within each hydrogel condition group and thus give insight into whether cells were metabolically active at the time of testing.

Looking at the D7 results of CellTiter-Glo® (Figure 18), three significant differences can be observed. There was significantly more ATP present in the 1 wt% HA soft (200 Pa) condition compared to the 0.1 wt% HA soft (200 Pa) condition. Also, a significant decrease was seen between day 1 and 7 for both the 0.1 wt% HA medium (400 Pa) stiffness condition and the 0.5 wt% HA soft (200 Pa) stiffness condition. The data also shows that the amount of ATP present in all conditions decreased between days 1 and 7, although not significantly. Looking at the 1 wt% HA conditions, as stiffness increased total ATP decreased. Finally, looking at the day 7 results, ATP increased with increasing HA concentration.

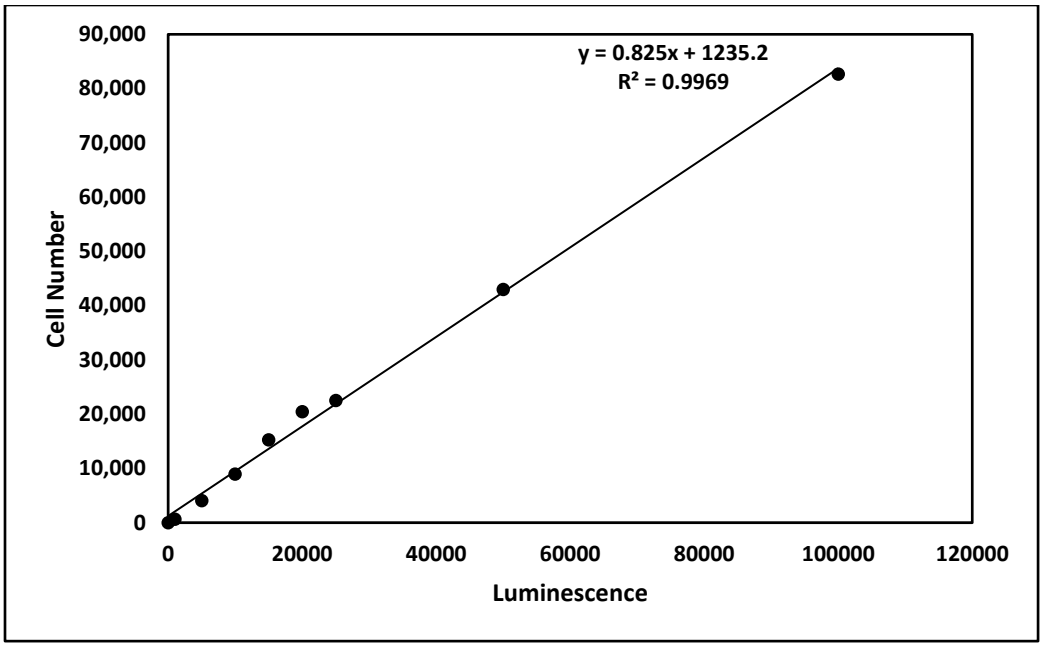


**Figure 17:** CellTiter-Glo® standard curve results from day 1 of encapsulation 2 plotting total cell number vs. luminescence as read from a BioTek plate reader.

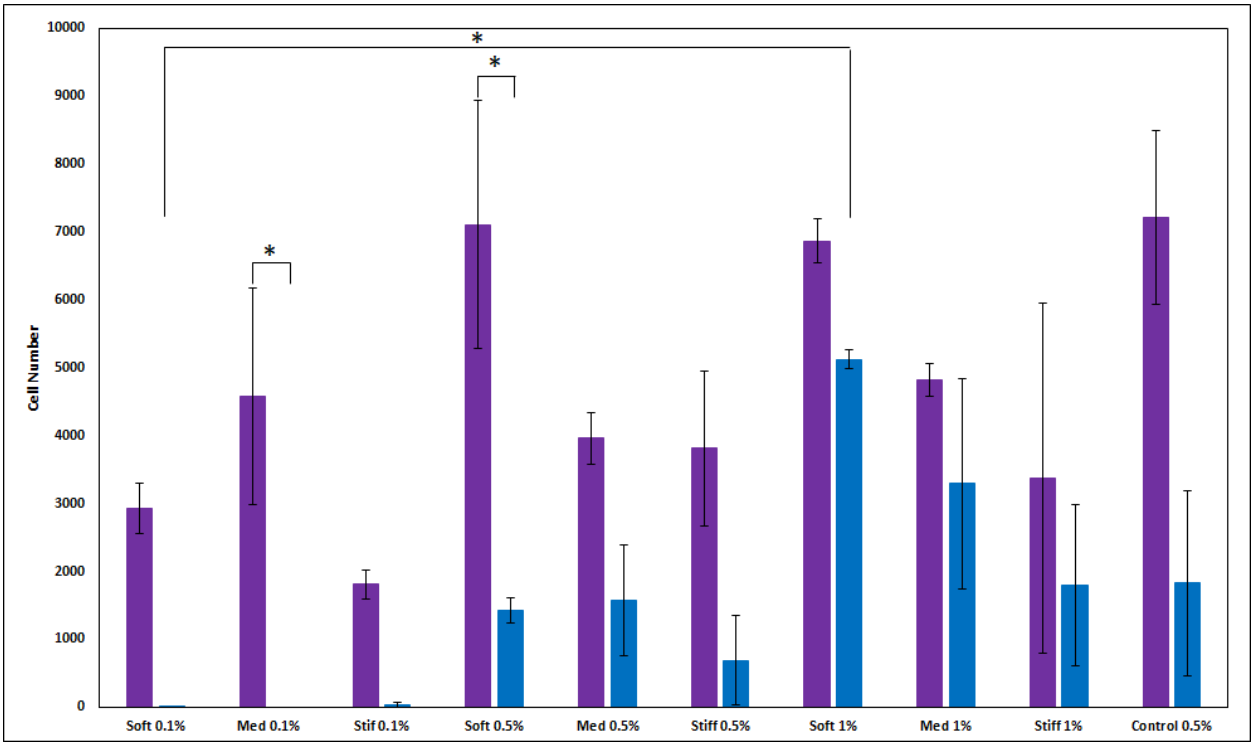


**Figure 18:** CellTiter-Glo® results are shown for each of the ten conditions **1A**: 200 Pa 0.1 wt% HA, **2A:** 400 Pa 0.1 wt% HA, **3A:** 800 Pa 0.1 wt% HA, **1B:** 200 Pa 0.5 wt% HA, **2B:** 400 Pa 0.5 wt% HA, **3B:** 800 Pa 0.5 wt% HA, **4B Control:** 150 Pa 0.5 wt% HA, **1C:** 200 Pa 1 wt% HA,

**2C:** 400 Pa 1 wt% HA, **3C:** 800 Pa 1 wt% HA. Days 1 (Purple) and 7 (Blue) are compared. (n=3) Error bars are standard error. * means $p < 0.05$

A DNA assay was used in conjunction with the CellTiter-Glo® results to create a more informed picture of what was going on at the two timepoints assessed (Figure 19). While this assay represents the total DNA, from both dead and alive cells, it gave an idea of overall cell population number and was compared to metabolic activity of the cell population. Statistical analysis determined that total DNA did not vary significantly between or within any groups. However, in all conditions there seemed to be more DNA present at day 7 compared to day 1.

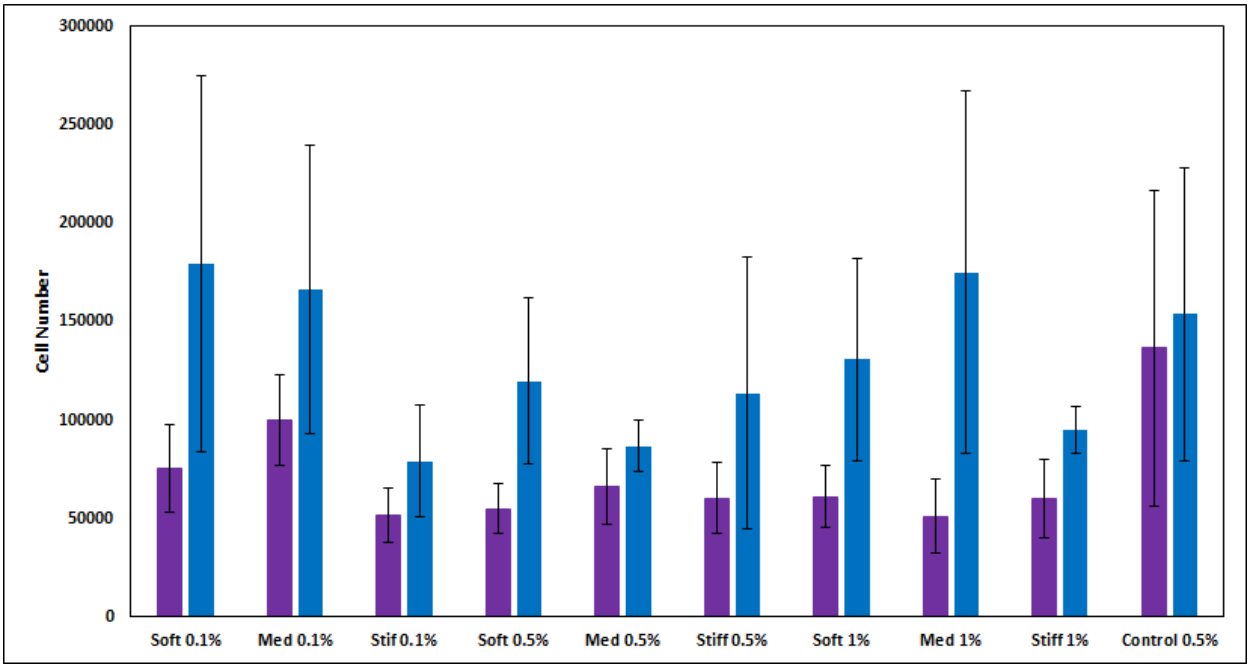


**Figure 19:** DNA Assay results are shown for each of the ten conditions **1A**: 200 Pa 0.1 wt% HA, **2A:** 400 Pa 0.1 wt% HA, **3A:** 800 Pa 0.1 wt% HA, **1B:** 200 Pa 0.5 wt% HA, **2B:** 400 Pa 0.5 wt% HA, **3B:** 800 Pa 0.5 wt% HA, **4B Control:** 150 Pa 0.5 wt% HA, **1C:** 200 Pa 1 wt% HA, **2C:** 400 Pa 1 wt% HA, **3C:** 800 Pa 1 wt% HA. Days 1 (Purple) and 7 (Blue) are compared. (n=3) Error bars are standard error * means $p < 0.05$

Interpreting these two sets of results together, it seems that all conditions led to an increased number of cells between day 1 and 7, but the metabolic activity was highest in the 1 wt% HA condition. Figure 20 graphs the total ATP divided by the total DNA as a percentage. This gives an idea of the percentage of cells that are alive. The control 0.5 wt% HA condition decreased in live cell percentage between day 1 and 7 meaning cells were dying off in this time span even in the control group. It appears that as HA concentration increased so did this percentage of live cells. The soft (200 Pa) stiffness 1 wt% HA group had a higher percentage of live cells at day 7 compared to all other groups.

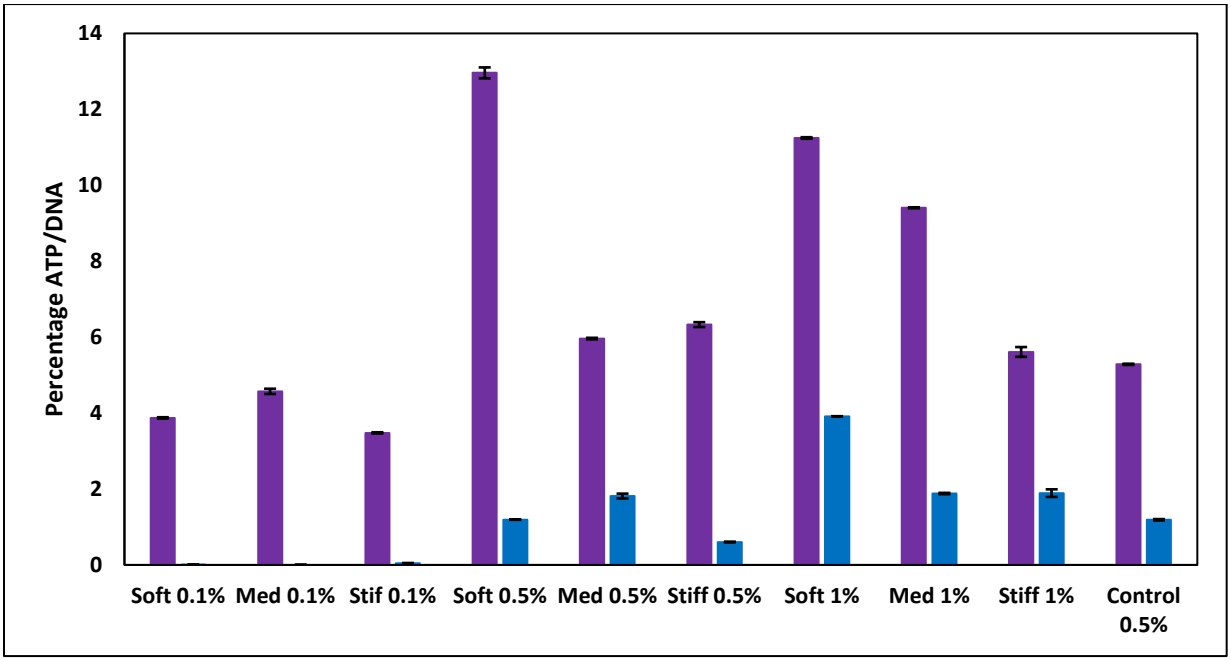


**Figure 20:** Percentage of ATP out of DNA is shown for each of the ten conditions **1A**: 200 Pa 0.1% HA, **2A:** 400 Pa 0.1% HA, **3A:** 800 Pa 0.1% HA, **1B:** 200 Pa 0.5% HA, **2B:** 400 Pa 0.5% HA, **3B:** 800 Pa 0.5% HA, **4B Control:** 150 Pa 0.5% HA, **1C:** 200 Pa 1% HA, **2C:** 400 Pa 1% HA, **3C:** 800 Pa 1% HA. Days 1 (Purple) and 7 (Blue) are compared. Error bars are standard error.

Proliferation was also investigated qualitatively at day 7 for all hydrogel conditions. Figure 21 shows that the stiff (800 Pa) condition had more Ki67 present compared to the soft

(200 Pa) and medium (400 Pa) stiffness groups. In Figure 22 a zoomed in view gives more insight into overall cell density. As seen in the viability studies, the 1 wt% HA condition shows more cell aggregation compared to the 0. 1wt% HA and 0.5 wt% HA groups. All groups show SOX2 meaning that at least a portion of each population are still NS/PCs. In addition, the 2B* group which was double-seeded at day 0 has the most Ki67 and SOX2 of any of the groups indicating that perhaps the higher seeding density improved paracrine signaling of the NS/PCs and led to a higher amount of proliferation within the one-week time span.

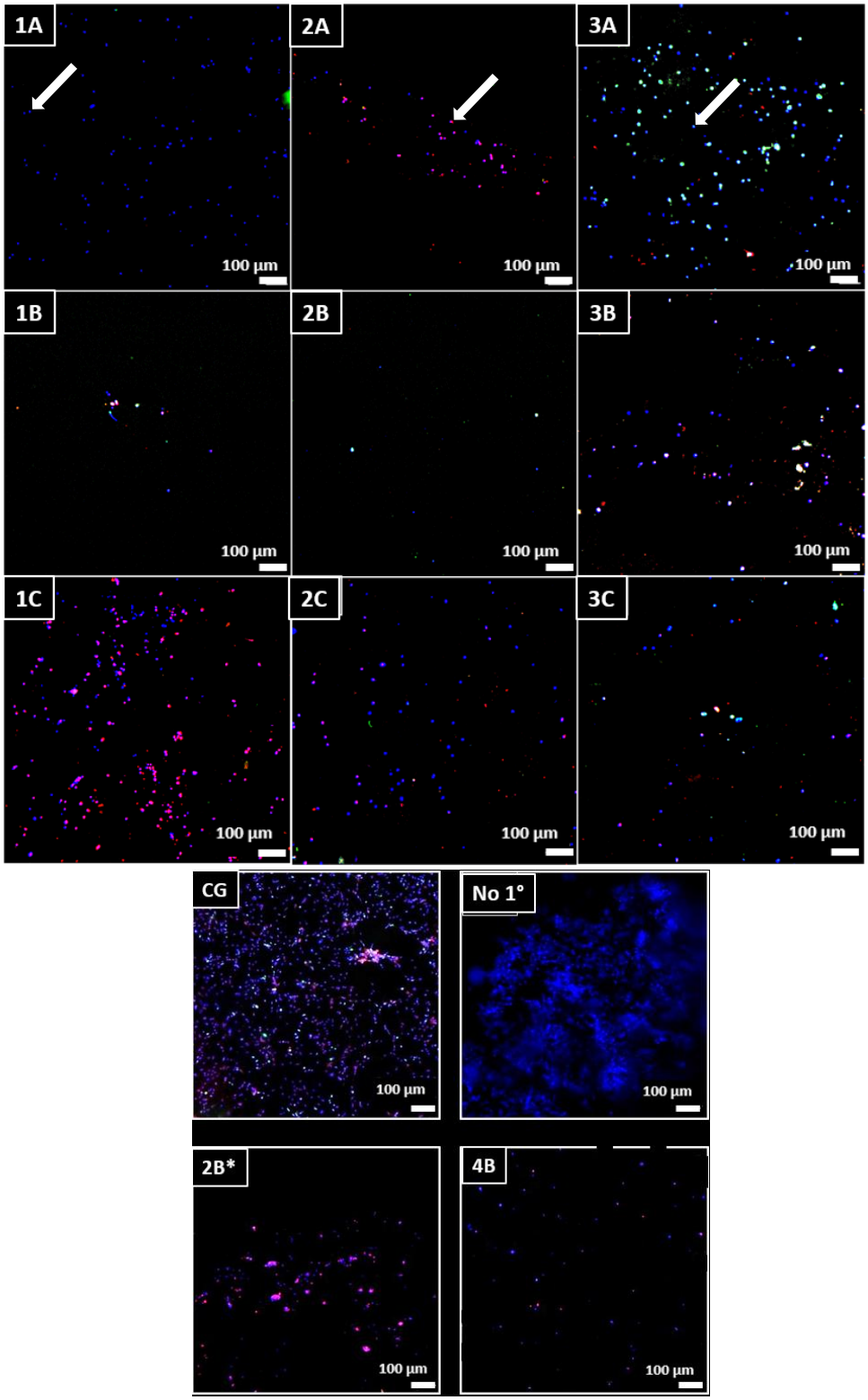


**Figure 21:** Immunostaining of SOX2, Ki67 and Hoescht to observe stem cellness and proliferation. Images shown are 18 µm slices of hydrogels sectioned after day 7 onto slides (Top). Arrows from left to right highlight a cell staining positive for Hoescht only, a cell staining

positive for Hoescht and SOX2 and a cell staining positive for Hoescht and Ki67. Controls (Bottom) include coverglass, coverglass with no primary antibodies 4B and 2B* which had the same formulation as 2B, but was used to compare a seeding density of 200k cells to the otherwise used 100k cells per hydrogel. Scale bars are 100 µm.

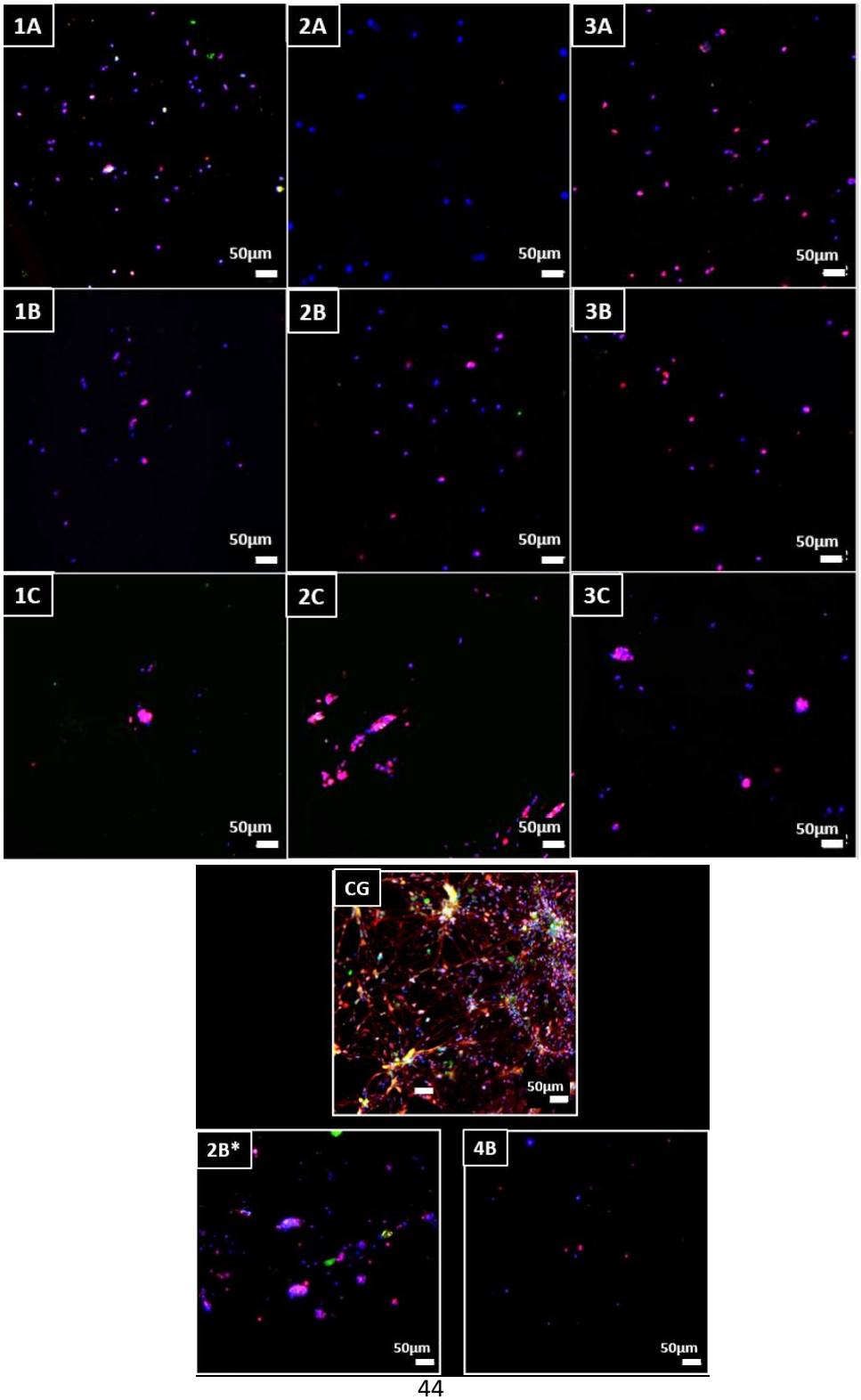

**Figure 22:** Immunostaining of SOX2, Ki67 and Hoescht to observe stem cellness and proliferation. Images shown are 18 µm slices of hydrogels sectioned after day 7 onto slides. Controls include coverglass, 4B and 2B* which had the same formulation as 2B, but was used to compare a seeding density of 200k cells to the otherwise used 100k cells per hydrogel. Scale bars are 50 µm.

### 3.4.4 Differentiation

Starting with the qualitative assessment, Figures 23 and 24 show immunostaining for differentiation markers in hydrogel sections (18 µm). An obvious increase in DCX is seen in the 0.1 wt% HA soft (200 Pa) stiffness group as compared to the others. It is difficult to ascertain comparative populations within the merged channel images, so the following three figures (25, 26 and 27) show the channels (PDGFRα, DCX and GFAP) separated with only Hoescht. Figure 25 demonstrates that PDGFRα is present in all groups, however there seems to be an increased amount in the 0.5 wt% HA groups as well as the low (200 Pa) and medium (400 Pa) stiffness 0.1 wt% HA groups. Looking at Figure 26 there is more DCX present in the soft (200 Pa) and medium (400 Pa) stiffness groups as compared to the stiff group (800 Pa). Comparing figure 27 to figures 26 and 25, there is more GFAP than DCX in the stiff conditions (800 Pa). There is also the least GFAP in relation to total cell number in the 0.5 wt% HA soft (200 Pa) stiffness group and the 1 wt% HA stiff (800 Pa) group.

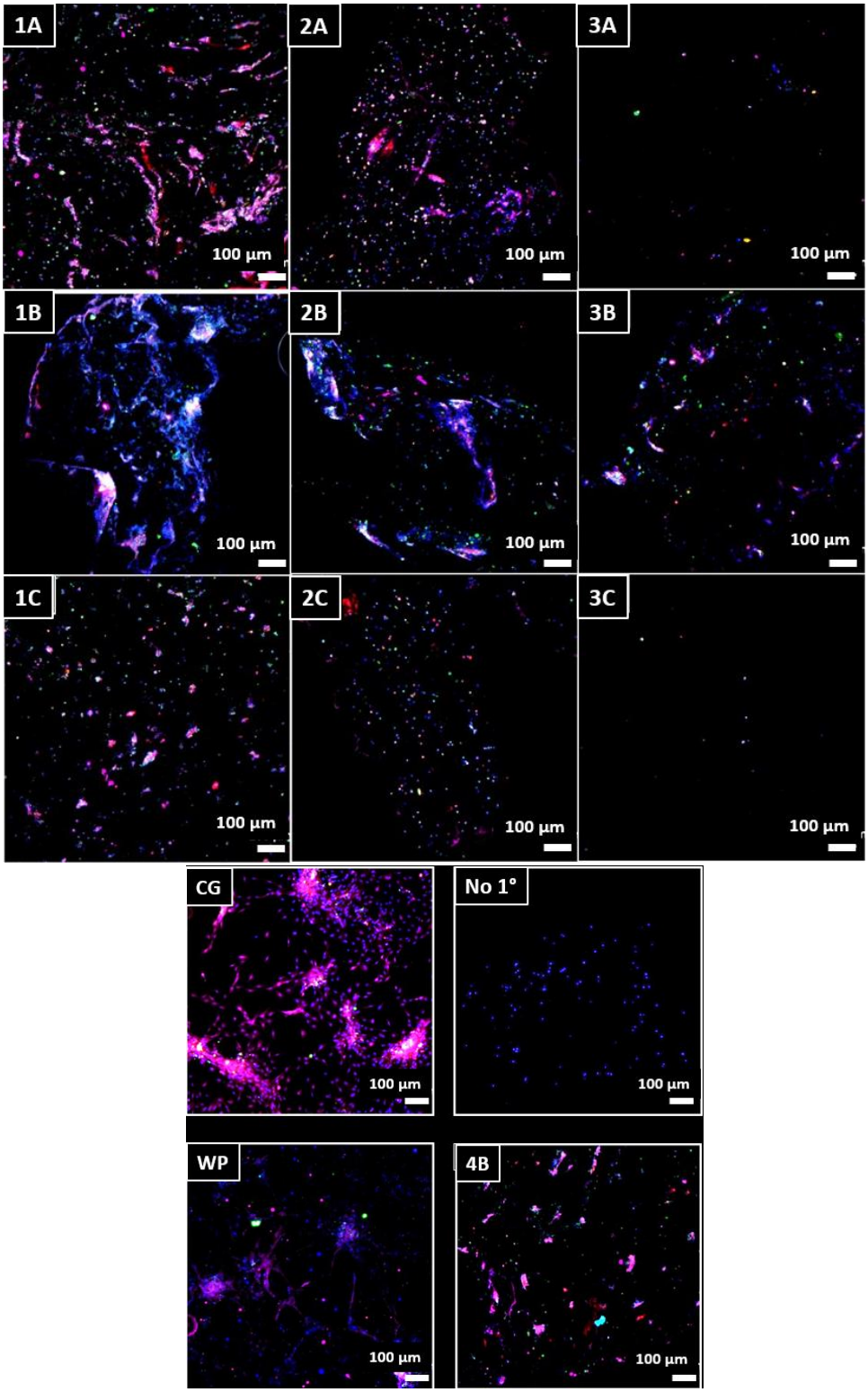


**Figure 23:** Immunostaining of PDGFRα, DCX, GFAP and Hoescht to observe differentiation. (Top) Images shown are 18 µm slices of hydrogels sectioned after day 14 onto slides. (Bottom)

Controls include coverglass, coverglass with no primary antibodies, well plate and 4B. Scale bars are 100 µm.

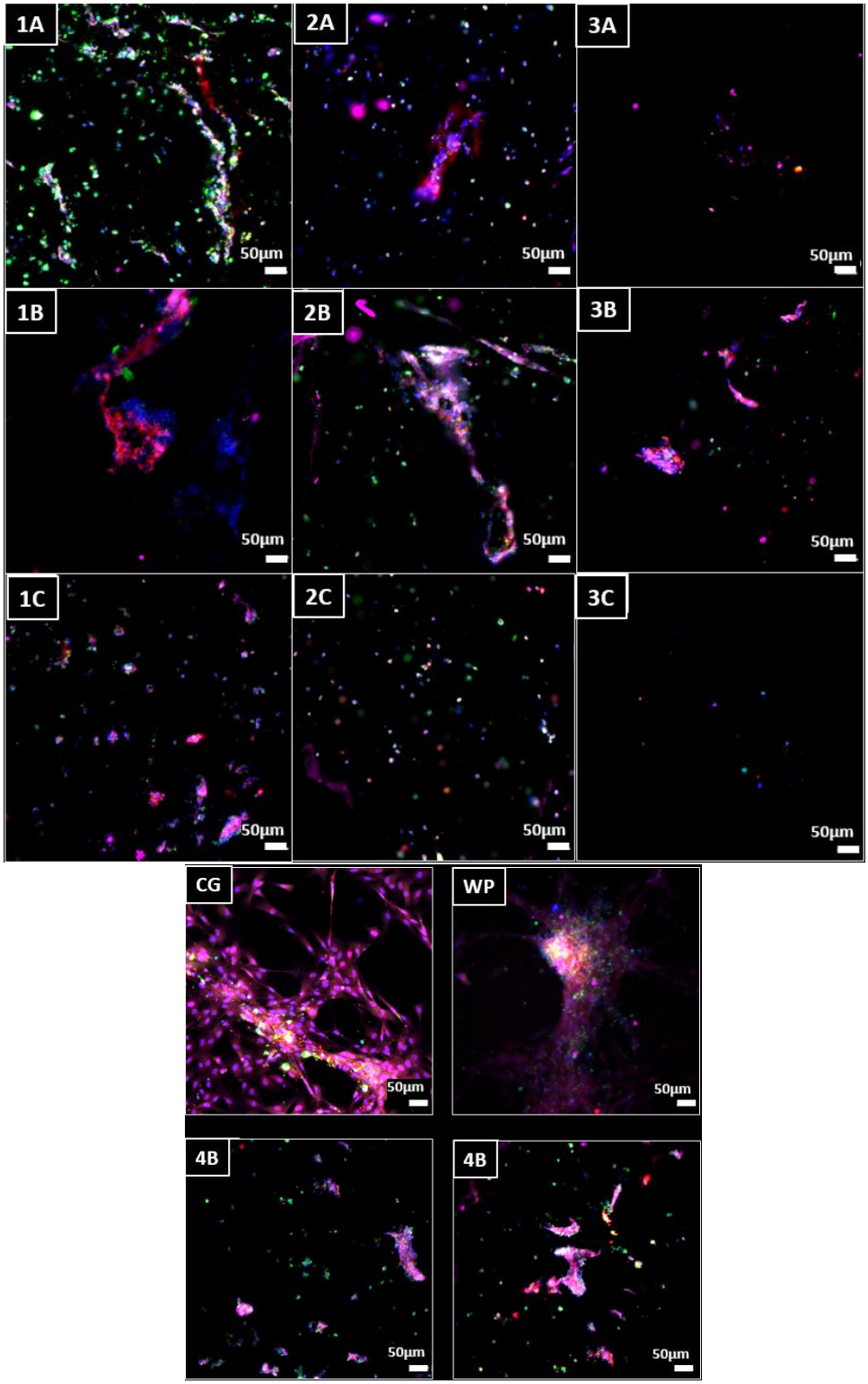

**Figure 24:** Immunostaining of PDGFRα, DCX, GFAP and Hoescht to observe differentiation. (Top) Images shown are 18 µm slices of hydrogels sectioned after day 14 onto slides. (Bottom) Controls include coverglass, well plate and 4B. Scale bars are 50 µm.

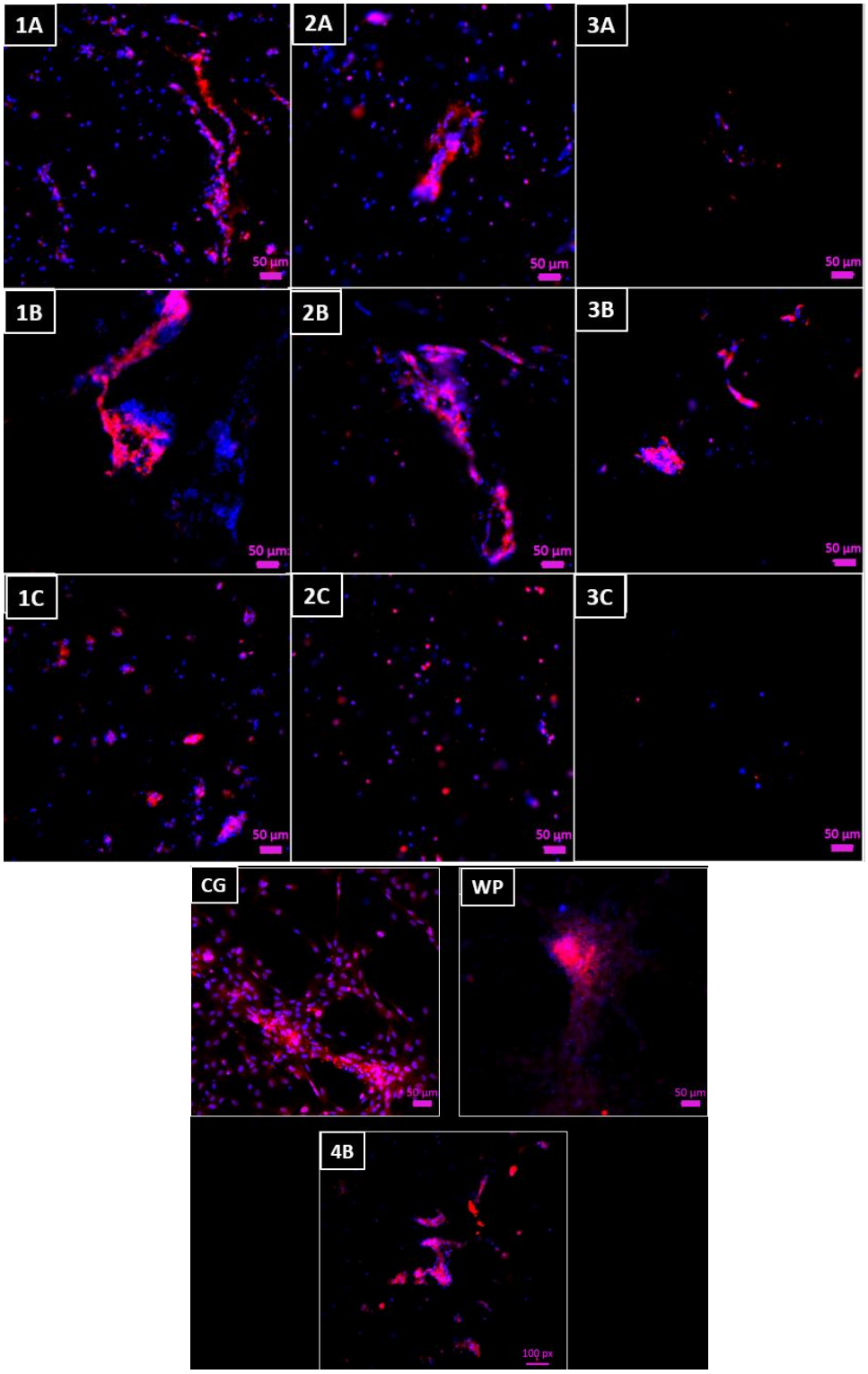

**Figure 25:** Immunostaining of PDGFRα and Hoescht to observe differentiation. (Top) Images shown are 18 µm slices of hydrogels sectioned after day 14 onto slides. (Bottom) Controls include coverglass, well plate and 4B. Scale bars are 50 µm.

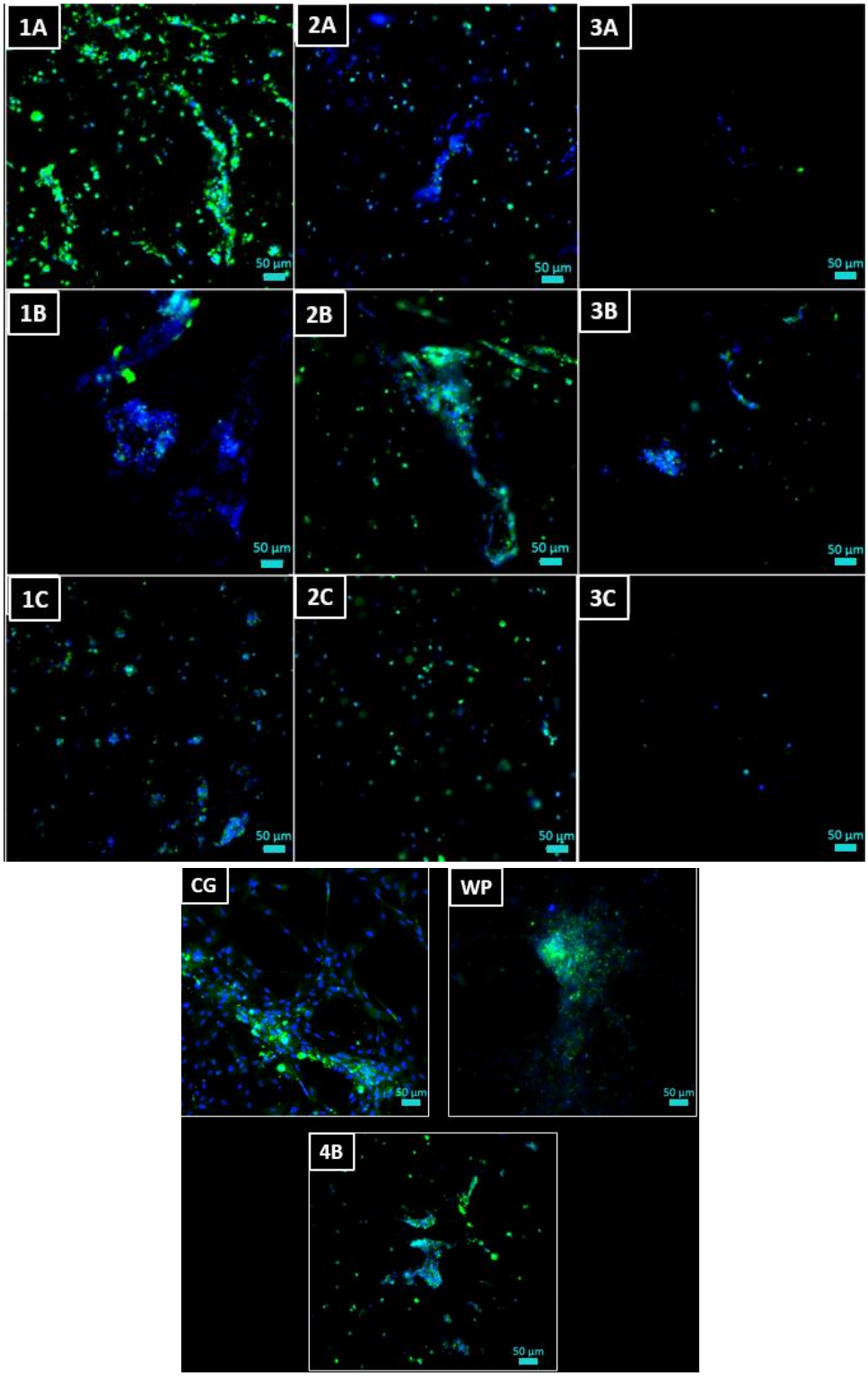

**Figure 26:** Immunostaining of DCX and Hoescht to observe differentiation. (Top) Images shown are 18 µm slices of hydrogels sectioned after day 14 onto slides. (Bottom) Controls include coverglass, well plate and 4B. Scale bars are 50 µm.

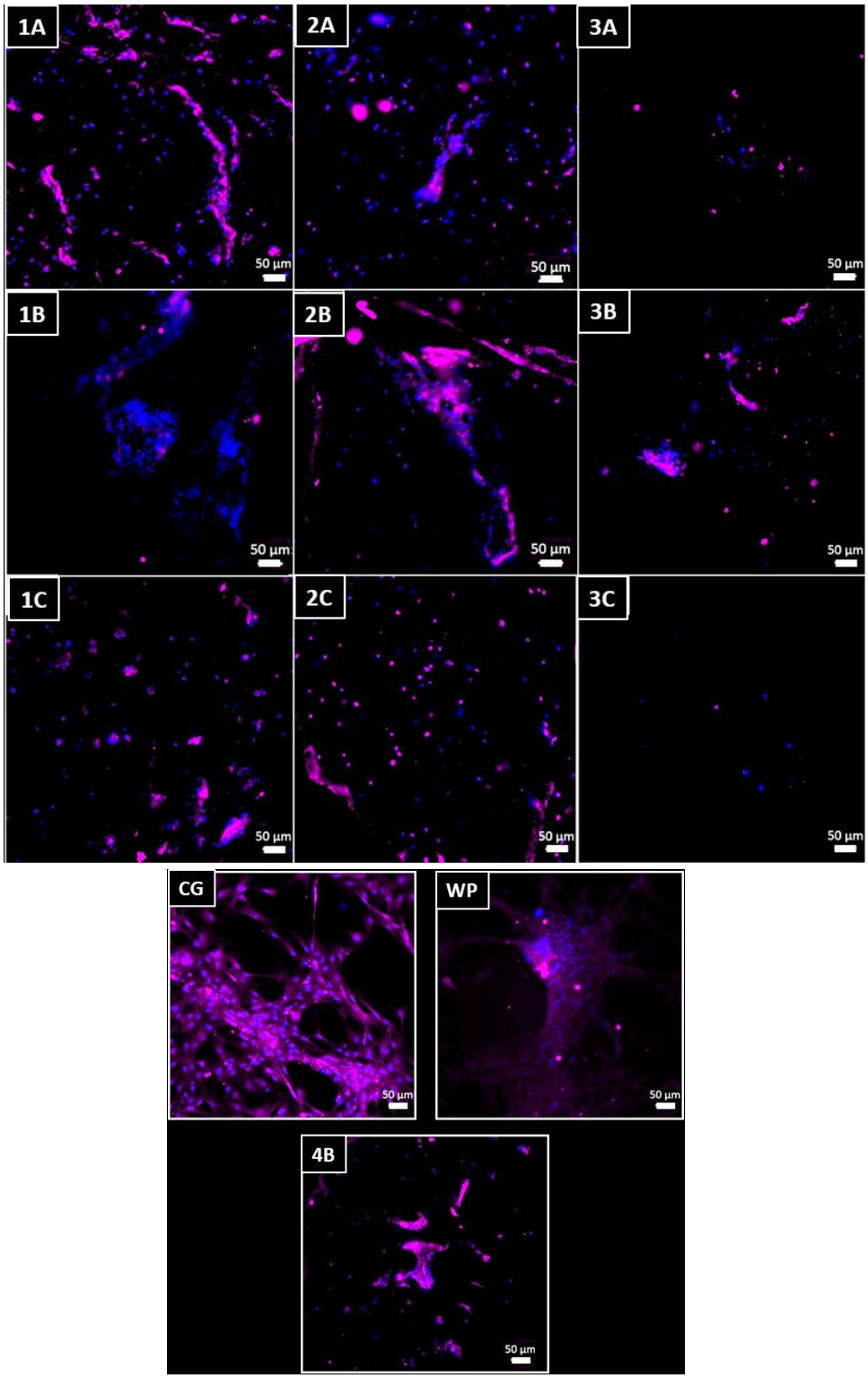

**Figure 27:** Immunostaining of GFAP and Hoescht to observe differentiation. (Top) Images shown are 18 µm slices of hydrogels sectioned after day 14 onto slides. (Bottom) Controls include coverglass, well plate and 4B. Scale bars are 50 µm.

While immunostaining sections of hydrogels is a good qualitative method for understanding the varied neural cell populations within these hydrogels, each section shown here only represents about 0.01% of the total volume of the hydrogels (0.45 $mm^3$ / 39.25 $mm^3$). For this reason, whole hydrogel staining was also performed and imaged on a Leica SP-5 Blue confocal microscope to assess 100 µm z-stacks composed of 25 (4µm) slices. This imaging provided a different perspective on the neural cell populations within each hydrogel condition and a method of comparison for the qualitative assessment.

Figure 28 shows a stacked image of all 25 (4 µm) z-stacks compared across groups. In agreement with the 2D staining, the 0.5 wt% HA medium (400 Pa) stiffness group showed a higher population of DCX positive cells. There was also more DCX present in the low (200 Pa) and medium (400 Pa) stiffness groups as compared to the high stiffness (800 Pa) group. Conversely, in accordance with the 2D staining there was more GFAP than DCX in the 1 wt% HA Stiff (800 Pa) group. This figure also includes a link to videos of the 3D hydrogel images spinning 360° and separated by channel. When viewed in this manner it is obvious that the 0.1 wt% and 0.5 wt% HA stiff (800 Pa) groups as well as the 4B control group had more GFAP than any other group while the 0.1 wt% HA soft (200 Pa), 0.5wt % HA medium (400 Pa) stiffness group and 4B control group had more DCX as compared to the other groups.

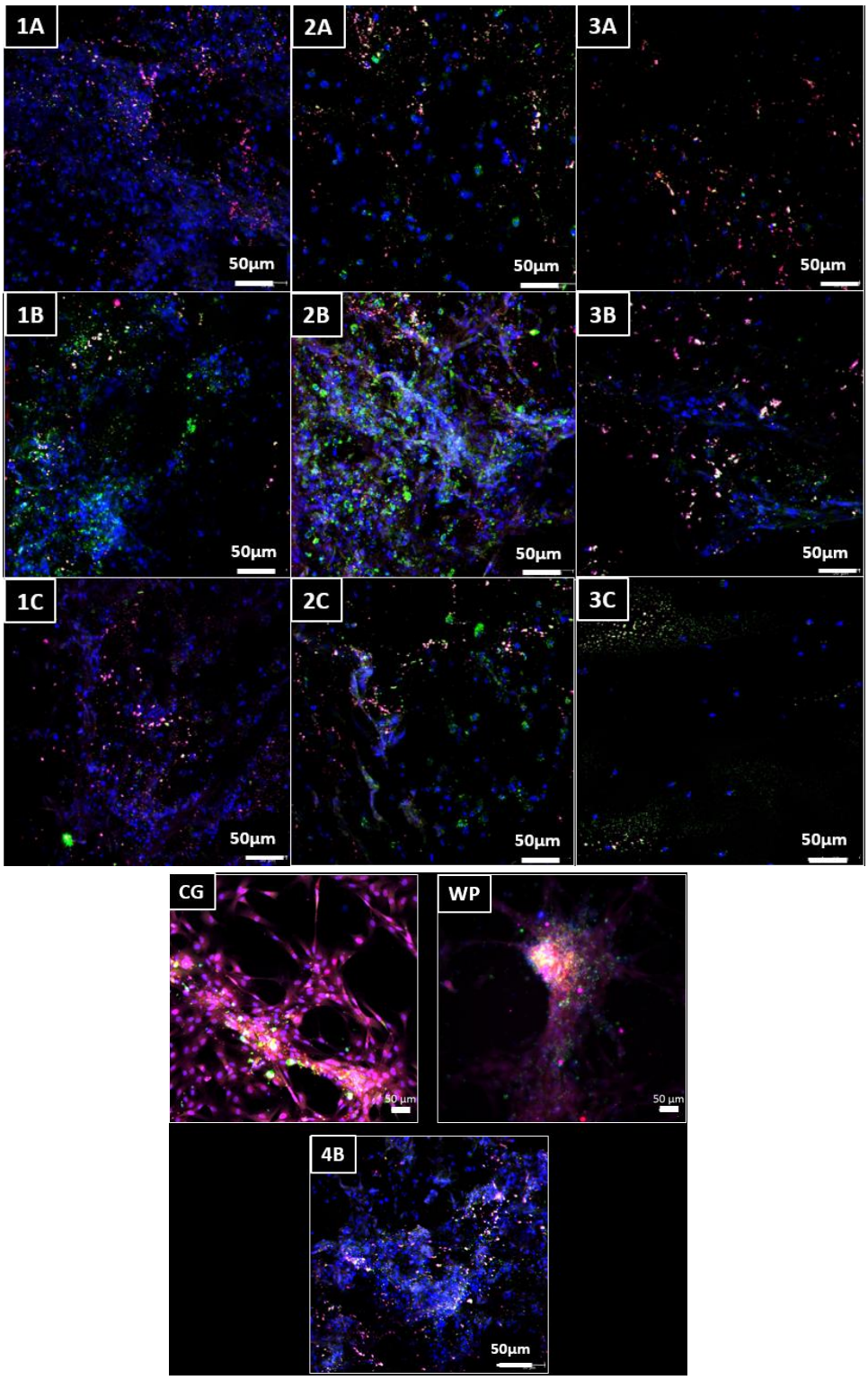


**Figure 28:** Immunostaining of PDGFRα, DCX, GFAP and Hoescht to observe differentiation. (Top) Images shown are 100 µm stacks of 25 (4 µm) z-slices of hydrogels fixed after day 14.

(Bottom) Controls include coverglass, well plate and stack of 4B z-slices. Scale bars are 50 µm. **Follow this link to see 3D videos of these image stacks separated by channel.

**Quantitative PCR**

qPCR was performed as a quantitative assessment for differentiation (Figure 29), investigating the same primers used in immunostaining (PDGFRα and GFAP) and one substitute of MAP2 in place of DCX. These results indicate that there were more of all population types in the 0.5 wt% and 1 wt% HA soft (200 Pa) stiffness group and 4B control groups (150 Pa) as compared to the standardized group (1A). These three groups also showed increased amounts of SOX2 above the other groups. Trace amounts of GFAP were seen in the 0.5 wt% and 1 wt% HA stiff (800 Pa) and 4B control groups. Overall, amount of DCX and PDGFRα decreased with increased stiffness of the hydrogels. There was also a clear increase in PDGFRα within the soft (200 Pa) stiffness groups of the 0.5 wt% and 1 wt% HA and 4B control group.

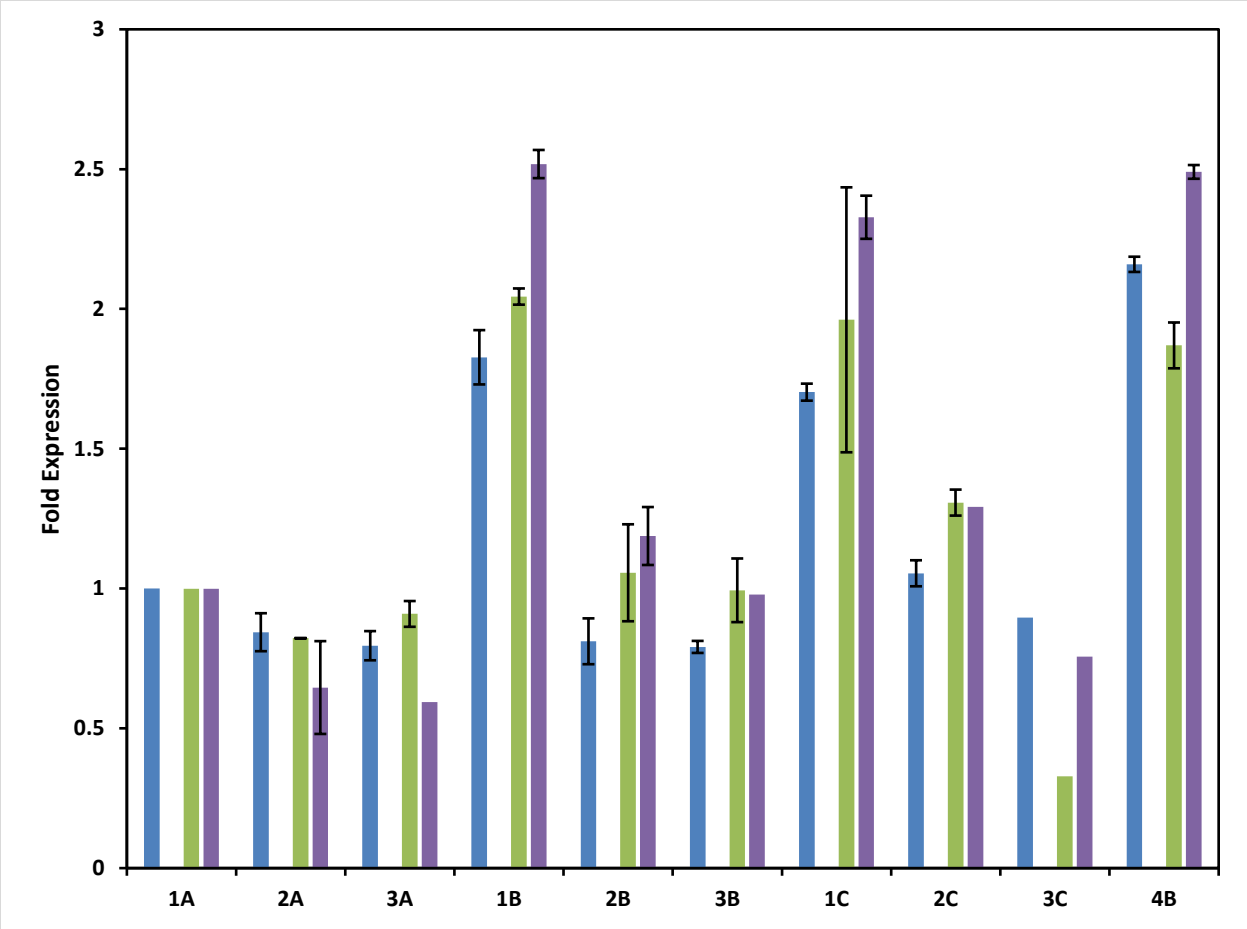


**Figure 29:** qPCR results shown as expression fold change compared to group 1A. SOX2, MAP2 and PDGFRα are shown. **1A**: 200 Pa 0.1% HA, **2A:** 400 Pa 0.1% HA, **3A:** 800 Pa 0.1% HA, **1B:** 200 Pa 0.5% HA, **2B:** 400 Pa 0.5% HA, **3B:** 800 Pa 0.5% HA, **4B Control:** 150 Pa 0.5% HA, **1C:** 200 Pa 1% HA, **2C:** 400 Pa 1% HA, **3C:** 800 Pa 1% HA. Day 14 results are compared across groups (n=1). Error bars are standard deviation. Bars without error were not tested in duplicate.

**Statistical Analysis**

For both CellTiter-Glo® and the DNA assay error bars represent standard error of the mean and were calculated by first finding the averages of the three proliferation encapsulations. Standard deviation was then calculated and this value was divided by the square root of 'n' to produce error bar values. Statistical analysis was then performed using a three-way Analysis of Variance (ANOVA). The dependent variable was cell number, while the three independent

variables compared were time (day 1 vs. day 7), HA concentration and stiffness. Statistical analysis was performed using GraphPad Prism 7.

Tukey's Test, a post hoc test that can be performed on ANOVA, was run using the same program to compare within and between every group in the analysis. The P value was set to 0.05 and any comparison that returned a value under the P value meant the null hypothesis was rejected and the groups were significantly different. For qPCR results, error bars were calculated as standard deviation from the mean. More repeats will have to be performed to analyze statistical differences between conditions for qPCR.

### 3.5 Discussion:

*Rheology*

After several iterations of rheological characterization (>20) I have concluded that it takes much skill and practice to make HA-based hydrogels with consistent mechanical properties. Even once I had become proficient, the variation from batch to batch of HA-SH led to a trial and error effort each time to determine the proper total thiol to achieve the desired stiffness groups for this research. As was shown in the results section (Figure 14), mechanical properties varied between batches of HA-SH even when the total thiol and thiol to maleimide ratio was maintained. I believe this was due in part to the level of uncertainty involved in assessing thiolation percentage using Ellman's test and Proton NMR. Although the two tests agreed on the range of thiolation there was up to a 0.5% error meaning that a 4% thiolated batch of HA could really be 3.5% or 4.5% thiolated. This led to uncertainty in the total thiol calculations due to the HA-SH contributions. There was also uncertainty introduced from the rheological characterization. However, in the end it was

possible to consistently achieve the desired stiffnesses (200, 400 and 800 Pascal) for each batch of HA-SH used in this study across all HA concentrations (0.1 wt%, 0.5 wt% and 1 wt%).

When considering the basic architecture of the HA-based hydrogels, an important consideration is that a higher thiolation percentage of HA-SH likely leads to the formation of a greater number of disulfide bonds from HA-SH binding to itself compared to lower thiolation percentage batches. In lower thiolation percentage batches of HA-SH, the architecture is mostly contributed by maleimide-sulfide crosslinks between both HA-SH/PEG-SH and PEG-Mal. This difference in molecular binding schemes is also a likely cause of variations in the stiffness of gels even when total thiol was maintained between HA-SH batches.

*Viability*

NS/PC survival was assessed using immunostaining which provided a qualitative measurement of relative viability within each hydrogel condition. At the day 7 timepoint it seemed that the 0.1 wt% HA hydrogels induced more cell death compared to other HA concentrations as was demonstrated by the presence of more cParp in these sections. This makes sense in that the 0.1 wt% HA condition was the group included to represent the effects of a hydrogel with relatively no HA, but rather a mostly PEG-crosslinked hydrogel. Since HA is known to interact with NS/PCs and is a part of their native environment, the lack of it might indeed lead to more apoptotic behavior. This was further confirmed in that the 1 wt% HA groups had similar population numbers to the other groups but relatively no cParp present. These high HA concentration groups also had the most aggregation of cells, which relates to an increase in paracrine signaling in which cells communicate to initiate proliferative behavior.

Live/Dead staining of the whole hydrogels provided a secondary method for qualitative

evaluation of NS/PC viability within the hydrogel conditions. These stains showed incongruous results to that of cParp staining in that there was a greater percentage of dead cells observed in the 1 wt% HA conditions compared to the other HA concentrations. It was also seen that the 0.5 wt% HA group contained the largest populations of live cells and smallest percentage of dead cells. I believe the live/dead stains were more indicative of what was really going on since they represented much more of the overall hydrogel, however all the immunostaining provided only a qualitative assessment of NS/PC viability. So, in conclusion the 0.5 wt% HA groups led to the greatest NS/PC viability and this viability decreased with stiffness leading to the most viable groups being 0.5 wt% HA soft (200 Pa) and medium (400 Pa) stiffness groups.

*Proliferation*

For the quantitative assessment of proliferation, a combination of CellTiter-Glo® (overall ATP) and a DNA assay (total DNA) were performed. The CellTiter-Glo® results showed that the total amount of ATP increased with HA concentration while the total ATP generally decreased with stiffness. This implies that at day 7 the high HA concentration groups were most metabolically active as well as the softer conditions. The DNA assay showed relatively more total DNA in the 1 wt% HA group from day 1 to day 7. The soft (200 Pa) and medium (400 Pa) stiffness groups had the most DNA present in the 0.1 wt% and 1 wt% HA. Although this conflicts with the immunostaining results in which the 0.5 wt% HA group showed the most viable cells, the total DNA represented in this study might be accounting for more dead than alive cells. This explanation seemed to agree with the ATP/DNA data which showed that the percentage of live cells increased with increasing HA concentration.

The qualitative assessment of the data assessed SOX2, a marker for NS/PCs in their stem cell stage and Ki67 a marker for proliferation. SOX2 was expressed in every group as would be expected after seven days in proliferation media. Ki67 seemed much more present in the stiffer (800 Pa) groups and decreased as HA concentration increased. Spinal cord stiffness is known to be in the range of 0.5-1 kPa, which puts the stiff condition tested in this research (800 Pascal) right in the middle of this range. This is potentially why the cells seem to proliferate most in this stiffer condition. In conclusion, all conditions retained their stem cellness, but the high HA condition was most metabolically active especially in the softest condition.

*Differentiation*

Starting with the qualitative assessment, higher populations of cells were observed in the soft (200 Pa) and medium (400 Pa) stiffness groups as compared to the stiff (800 Pa) group. The 0.5 wt% HA groups had the most PDGFRα staining present compared to other HA concentrations relating to the highest populations of oligodendrocytes. There was also more of this staining observed in the 0.1 wt% HA conditions as compared to the 1 wt% HA and all three groups showed PDGFRα staining was inversely proportional to stiffness of the hydrogels. My hypothesis was that oligodendrocyte populations would be more prevalent in low HA conditions which was proven correct keeping in mind that the 0.1 wt% HA condition had relatively no HA present. In terms of the stiffness effects, the most oligodendrocytes were seen in the softer (200 Pa) stiffness conditions and these populations decreased with increased stiffness.

DCX staining represents neuronal populations and was most pronounced in the soft (200 Pa) and medium (400 Pa) stiffness hydrogels. There was also most DCX observed in the soft (200 Pa) 0.1 wt% HA conditions, followed by medium (400 Pa) 0.5 wt% and 1 wt% HA conditions. This confirmed my hypothesis that the neuronal populations would be more prevalent

in softer environments. However, I had also hypothesized that increasing HA concentration would directly relate to higher neuronal cell populations and this was not shown by the qualitative results.

GFAP, a marker of astrocytes, was seen in greater amounts than neuronal or oligodendrocyte markers in the stiff (800 Pa) conditions, which agreed with my hypothesis that astrocyte populations would be seen more in a stiffer environment. However, some GFAP was also seen in the soft (200 Pa) and medium (400 Pa) stiffness conditions and there was no clear relationship of HA concentration to astrocyte differentiation. The 3D hydrogel imaging performed using confocal microscopy agreed with the 2D staining and provided more information about the neural cell populations within each hydrogel condition. The 3D staining showed the stiffer (800 Pa) 0.1 wt% and 0.5 wt% HA groups had the largest astrocyte populations compared to other groups, while the soft (200 Pa) 0.1 wt% HA and medium (400 Pa) 0.5 wt% HA had the largest neuronal populations. The 4B control (0.5 wt% HA 150 Pa) and 0.5 wt% HA medium (400 Pa) stiffness groups showed the largest amounts of all three neural populations.

The quantitative assessment, achieved through qPCR, was also in agreement with the 2D and 3D staining showing that there was the largest amount of all three populations of neural cells present in the 4B control (0.5 wt% HA 150 Pa) condition. Although not shown in the graphs, the stiff (800 Pa) 0.1 wt% and 0.5 wt% HA and 4B control group all showed trace amounts of GFAP RNA while the other groups had none. DCX and PDGFRα decreased with increased stiffness of the hydrogels. There was also markedly more PDGFRα within the 0.5 wt% and 1 wt% HA groups as compared to the 0.1 wt% HA in the medium (400 Pa) stiffness group. This disproved my hypothesis that oligodendrocyte population number would be inversely proportional to HA concentration, because based on the quantitative results it is just the opposite. SOX2, a marker of

neural stem cellness was present in all groups, but was up-regulated in the soft (200 Pa) stiffness groups to include 4B, the softest (150 Pa) condition.

In conclusion, more neuronal populations were found in soft (200 Pa) and medium (400 Pa) stiffness gels as compared to stiff (800 Pa) gels while more astrocytes were seen in stiffer gels. There was also an inversely proportional relationship between HA concentration and oligodendrocyte population.

### 3.6 Conclusion and Future Directions:

It was very encouraging to see that my research aligned with similar past research of human NS/PC population studies. This work showed that the 0.5 wt% HA concentration hydrogels in combination with a medium (400 Pa) stiffness value was conducive to all three neural cell populations studied here, neuronal, oligodendrocyte and astrocyte. This research also showed that neuronal populations are seen in greater amounts in 200 Pa and 400 Pa stiffness microenvironments as compared to stiffer (800 Pa) microenvironments. Oligodendrocyte populations were increased in the 0.1 wt% and 0.5 wt% HA concentration environments and astrocyte populations were increased in stiffer (800 Pa) environments. This information is very valuable in that the goal of SCI repair is to be able to introduce specific neural cell populations to the injury cite using an injection technique that will lead to cell viability after invasive administration. Since neurons and oligodendrocytes are likely most valuable for SCI repair therapeutics, a wise next step would be to further explore 200 Pa and 400 Pa stiffness hydrogels with a 0.1 wt% or 0.5 wt% HA concentration. This research has helped to elucidate microenvironmental conditions that induce greater percentages of specific neural cells.

Future directions include more repeats of the differentiation stage of the experiment to make conclusive statistical interpretations of the quantitative assessment. Other steps include taking the qualitative information from immunostaining and calculating the total number of cells present compared to cells expressing each differentiation marker to have more quantitative information. Another future step is to test diffusion within the hydrogels to confirm a similar value between conditions, which relates to a consistent hydrogel architecture. This can be accomplished using FITC-labeled Dextran. I also plan to carry this research into my future PhD studies in which I will culture the neuronal and oligodendrocyte populations within the HA-based hydrogels and administer them to the rodent spinal cord in both a sham and injury setting.

## REFERENCES


1. Stenudd M, Sabelström H, Frisén J. Role of Endogenous Neural Stem Cells in Spinal Cord Injury and Repair. *JAMA Neurol.* 2015;72(2):235–237. doi:10.1001/jamaneurol.2014.2927

2. Spinal Cord Injury Information Page. (n.d.). Retrieved June/July 2018, from https://www.ninds.nih.gov/disorders/all-disorders/spinal-cord-injury-information-page

3. Spinal Cord Injury Information Page. (n.d.). Retrieved June/July, 2018, from https://www.ninds.nih.gov/disorders/all-disorders/spinal-cord-injury-information-page

4. Kennea, N. L., & Mehmet, H. (2002). Neural Stem Cells. *Journal of Pathology*,*197*(4). doi:10.1007/springerreference_33916

5. Healthcare industry. (2011, July 25). Retrieved from https://www.gesundheitsindustrie-bw.de/en/article/dossier/cell-culture-technology-it-all-started-with-frog-nerve-fibres/

6. Edmondson, R., Broglie, J. J., Adcock, A. F., & Yang, L. (2014). Three-Dimensional Cell Culture Systems and Their Applications in Drug Discovery and Cell-Based Biosensors. *Assay and Drug Development Technologies*, *12*(4), 207–218. http://doi.org/10.1089/adt.2014.573

7. Agarwal, S., Wendorff, J. H., & Greiner, A. (2008, September 24). Use of electrospinning technique for biomedical applications. Retrieved from https://www.sciencedirect.com/science/article/pii/S0032386108007994

8. Selyanin, M. A., Boykov, P. Y., Khabarov, V. N., & Polyak, F. (n.d.). The History of Hyaluronic Acid Discovery, Foundational Reserch and Initial Use. Retrieved from https://onlinelibrary.wiley.com/doi/10.1002/9781118695920.ch1

9. Kim, J., Park, Y., Tae, G., Kyu, B. L., Chang, M. H., Soon, J. H., … Sun, K. (2009). Characterization of low-molecular-weight hyaluronic acid-based hydrogel and differential stem cell responses in the hydrogel microenvironments. *Journal of Biomedical Materials Research - Part A*, *88*(4), 967–975. https://doi.org/10.1002/jbm.a.31947

10. Stukel Jessica M. and Willits Rebecca Kuntz.Tissue Engineering Part B: Reviews.Jun 2016.ahead of print. http://doi.org/10.1089/ten.teb.2015.0380

11. Lin, C. M., Lin, J. W., Chen, Y. C., Shen, H. H., Wei, L., Yeh, Y. S., Chiu, W. T. (2009). Hyaluronic acid inhibits the glial scar formation after brain damage with tissue loss in rats. *Surgical Neurology*, *72*(SUPPL. 2). https://doi.org/10.1016/j.wneu.2009.09.004

12. Su, W., Foster, S. C., Xing, R., Feistel, K., Olsen, R. H. J., & Summer, F. (2017). CD44 and Hyaluronan Regulate Adult Hippocampal Neural Stem Cell Quiescence and Differentiation, 1–24. http://doi.org/10.1074/jbc.M116.774109

13. Leipzig, N. D., & Shoichet, M. S. (2009). Biomaterials The effect of substrate stiffness on adult neural stem cell behavior. *Biomaterials*, *30*(36), 6867–6878. http://doi.org/10.1016/j.biomaterials.2009.09.002

14. Hellemond, V., & Giezen, V. Der. (2014). Animal Evolution : Looking for the First Nervous System, 655–658. http://doi.org/10.1016/j.cub.2014.06.036

15. Araque, A., & Navarrete, M. (2010). Glial cells in neuronal network function, 2375–2381. http://doi.org/10.1098/rstb.2009.0313

16. Brain Basics: Know Your Brain. (n.d.). Retrieved from https://www.ninds.nih.gov/Disorders/Patient-Caregiver-Education/Know-Your-Brain

17. B. (n.d.). Development of the Nervous System. Retrieved from https://courses.lumenlearning.com/boundless-ap/chapter/development-of-the-nervous-system/

18. El, G., D, M., GL, M., & H, S. (2003). Adult neural stem cells and repair of the adult central nervous system. *J Hematother Stem Cell Research*,*12*(6), 671-679. Retrieved from https://www.ncbi.nlm.nih.gov/pubmed/14977476.

19. Stukel, J. M., & Willits, R. K. (2015). Mechanotransduction of Neural Cells Through Cell–Substrate Interactions. *Tissue Engineering Part B: Reviews*, *22*(3), 173–182. http://doi.org/10.1089/ten.teb.2015.0380

20. *Fraser JR, Laurent TC, Laurent UB (1997). "Hyaluronan: its nature, distribution, functions and turnover". J. Intern. Med.* ***242*** *(1): 27–33.* PMID 9260563. doi:10.1046/j.1365-2796.1997.00170.x.

21. Mayor, R., & Theveneau, E. (2013). The neural crest. *Development (Cambridge, England)*, *140*(11), 2247–51. https://doi.org/10.1242/dev.091751

22. Chen, W., & Abatangelo, G. (1999). Function of hyaluronan in wound repair. *Wound Repair and Regeneration*, *7*, 79–89.

23. Lin, C. M., Lin, J. W., Chen, Y. C., Shen, H. H., Wei, L., Yeh, Y. S., … Chiu, W. T. (2009). Hyaluronic acid inhibits the glial scar formation after brain damage with tissue loss in rats. *Surgical Neurology*, *72*(SUPPL. 2). https://doi.org/10.1016/j.wneu.2009.09.004

24. Onoe, H., Kato-negishi, M., Itou, A., & Takeuchi, S. (2016). Differentiation Induction of Mouse Neural Stem Cells in Hydrogel Tubular Microenvironments with Controlled Tube

Dimensions, 1104–1111. http://doi.org/10.1002/adhm.201500903

25. Madl, C. M., & Heilshorn, S. C. (2018). Engineering Hydrogel Microenvironments to Recapitulate the Stem Cell Niche.

26. Rodell, C. B., Kaminski, A. L., & Burdick, J. A. (2013). Rational Design of Network Properties in Guest − Host Assembled and Shear-Thinning Hyaluronic Acid Hydrogels. http://doi.org/10.1021/bm401280z

27. Aguado, B. A., Mulyasasmita, W., Su, J., Ph, D., Lampe, K. J., Ph, D., … Ph, D. (2012). Improving Viability of Stem Cells During Syringe Needle Flow Through the Design of Hydrogel Cell Carriers, *18*, 806–815. http://doi.org/10.1089/ten.tea.2011.0391

28. Zalipsky, S., & Harris, J. (1997). Introduction to chemistry and biological applications of poly (ethylene glycol). *ACS Symposium Series*, (2), 1–13. https://doi.org/10.1021/bk-1997-0680.ch001

29. Wojcieszyn, J. W., Schlegel, R. A., Lumley-sapanski, J. K., & Jacobson, K. A. (n.d.). Studies on the Mechanism of Polyethylene Glycol-mediated Cell Fusion Using Fluorescent Membrane and Cytoplasmic Probes, (5).

30. Fenoli, C. R., & Bowman, C. N. (2014). The Thiol-Michael Addition Click Reaction: A Powerful and Widely Used Tool in Materials Chemistry. http://doi.org/10.1021/cm402180t

31. Spinal Cord Injury. (n.d.). Retrieved from https://www.urmc.rochester.edu/labs/nedergaard/projects/spinal-cord-injury.aspx

32. Silver, J., & Miller, J. H. (2004). Regeneration beyond the glial scar. *Nature Reviews Neuroscience*, *5*(2), 146–156. https://doi.org/10.1038/nrn1326

33. What emergency procedures occur following an SCI? (n.d.). Retrieved from https://www.christopherreeve.org/living-with-paralysis/newly-paralyzed/what-emergency-procedures-occur-following-an-sci

34. Rehabilitation. (n.d.). Retrieved from https://www.christopherreeve.org/living-with-paralysis/rehabilitation

35. Tulsky, D. S., Kisala, P. A., Victorson, D., Tate, D. G., Heinemann, A. W., Charlifue, S., … Cella, D. (2015). Overview of the Spinal Cord Injury – Quality of Life ( SCI-QOL ) measurement system, *38*(3), 257–269.

36. Su, W., Foster, S. C., Xing, R., Feistel, K., Olsen, R. H., Acevedo, S. F., . . . Sherman, L. S. (2017). CD44 and Hyaluronan Regulate Adult Hippocampal Neural Stem Cell Quiescence and Differentiation. *Journal of Biological Chemistry*,*292*(11), 4434-4445. doi:10.1074/jbc.m116.774109

37. Mih, J. D., Marinkovic, A., Liu, F., Sharif, A. S., & Tschumperlin, D. J. (2012). Matrix stiffness reverses the effect of actomyosin tension on cell proliferation. *Journal of Cell Science*, *125*(24), 5974–5983. http://doi.org/10.1242/jcs.108886

38. Engineering, M. (1996). The Mechanical Properties of the Human Cervical Spinal Cord In Vitro x i Upper grip plates Gauge length ~ S p i n a l cord sample ~ Adhesive, *24*, 67–74.

39. Seidlits, S. K., Khaing, Z. Z., Petersen, R. R., Nickels, J. D., Vanscoy, J. E., Shear, J. B., & Schmidt, C. E. (2010). Biomaterials The effects of hyaluronic acid hydrogels with tunable mechanical properties on neural progenitor cell differentiation. *Biomaterials*, *31*(14), 3930–3940. http://doi.org/10.1016/j.biomaterials.2010.01.125https://w

40. Mészár, Z., Felszeghy, S., Veress, G., Matesz, K., Székely, G., & Módis, L. (2008). Hyaluronan accumulates around differentiating neurons in spinal cord of chicken embryos. *Brain Research Bulletin*, *75*(2–4), 414–418. https://doi.org/10.1016/j.brainresbull.2007.10.052

41. Saha, K., Keung, A. J., Irwin, E. F., Li, Y., Little, L., Schaffer, D. V, & Healy, K. E. (2008). Substrate Modulus Directs Neural Stem Cell Behavior, *95*(November), 4426–4438. http://doi.org/10.1529/biophysj.108.132217

42. Back, S. A.  Et al. (2005). Hyaluronan accumulates in demyelinated lesions and inhibits oligodendrocyte progenitor maturation. *Nature Medicine*, *11*, 966-972.

43. Ellman's Test Protocol. (n.d.), (1998), 8972.

44. Winther, R., Jakob, Thorpe, Colin (2015). Quantification of Thiols and Disulfides. NIH Public Access, *1840*(2), 1–26. http://doi.org/10.1016/j.bbagen.2013.03.031.

45. Bart, J., Tiggelaar, R., Yang, M., Schlautmann, S., & Gardeniers, H. (2014). Room-temperature intermediate layer bonding for microfluidic devices Room-temperature intermediate layer bonding for microfluidic devices, (May). http://doi.org/10.1039/b914270c

46. Nguyen, H. X., Nekanti, U., Haus, D. L., Funes, G., Moreno, D., Kamei, N., … Anderson, A. J. (2014). Induction of Early Neural Precursors and Derivation of Tripotent Neural Stem Cells From Human Pluripotent Stem Cells Under Xeno-Free Conditions, *2783*, 2767–2783. http://doi.org/10.1002/cne.23604

47. T. (2016, July 19). Implementation of Promega's Dual Luciferase Reporter Assay System on Tecan's Spark 20M Multimode Reader. Retrieved from https://www.news-medical.net/whitepaper/20160719/Implementation-of-Promegae28098s-Dualc2adLuciferase-Reporter-Assay-System-on-Tecane28099s-Spark-20M-Multimode-Reader.aspx

48. Lim, H. J., Perera, T. H., Wilems, T. S., Ghosh, S., Zheng, Y., Azhdarinia, A., & Smith, L. A. (2016). Response to di-functionalized hyaluronic acid modification sites in rodent models of neural differentiation and spinal cord injury †. *Journal of Materials Chemistry B*, *4*, 6865–6875. http://doi.org/10.1039/C6TB01906D